Intrinsic Dynamics and Stability Properties of Size-Structured Pelagic Ecosystem Models

Ivan D. Lima (1), Donald B. Olson (2), and Scott C. Doney (1)

(1) National Center for Atmospheric Research
Climate and Global Dynamics Division
1850 Table Mesa Drive, Boulder CO, 80307, USA

(2) Rosenstiel School of Marine and Atmospheric Sciences
Division of Meteorology and Physical Oceanography
4600 Rickenbacker Causeway, Miami, FL 33149-1098, USA

February 1, 2001

Abstract

Although pelagic ecosystem models, coupled with ocean circulation models, are being widely used to quantify fluxes of nutrients and carbon in the ocean at regional and basin scales, relatively little work has been done on understanding their intrinsic dynamics independently of physical forcing. In this study, the dynamics of three common formulations for the NPZD class of models (nutrient, phytoplankton, zooplankton and detritus) using two different types of predation functional response are analyzed and compared. Our goal is to characterize the stability properties of this class of models with respect to variations in light and total nutrient concentrations. Despite important structural differences, the different model formulations all show asymptotic stable equilibria at low total nutrient concentrations and high to moderate light intensities and limit cycle oscillations at low light intensities and high total nitrogen concentrations. Limit cycles are formed through a Hopf bifurcation, as a phase lag develops between predator (Z_i) and prey (P_i or Z_{i-1}) due to a relatively sharp increase in the growth rate of the prey in relation to that of the predator. The use of variable preferences in the functional response provides a density-dependent mechanism that allows the system to self-regulate, increasing system stability considerably, but do not eliminate the instabilities completely. Instabilities occur at light and nutrient levels that correspond to those observed on the bottom of the euphotic zone near the nutricline, where the deep chlorophyll maximum is usually located. This suggests that the deep chlorophyll maximum might be dynamically unstable. This dynamical disequilibrium in species composition and the characteristically long transient times would allow species persistence in the presence of seasonal and mesoscale variations and provide a mechanism for species coexistence in the relatively homogeneous open ocean environment, thereby providing a potential solution for the “paradox of plankton”. In the multi-species models, the higher diversity of species (wider range of values for the biological parameters) allows biological activity (photosynthesis, grazing and predation) to occur under a

wider range of light and nutrient conditions resulting in higher primary and secondary production and lower nutrient concentrations at light intensities equivalent to those in the upper part of the euphotic zone, than in the single-species model.

Introduction

In the past decade, there has been renewed interest in marine ecosystem models (Fasham *et al.*, 1990; Eslinger, 1990; Moloney and Field, 1991; Olson and Hood, 1994; Doney *et al.*, 1996; Doney, 1999) due to the need to understand the effect of anthropogenic perturbations on the ocean carbon cycle. These models are now being coupled with ocean circulation models to quantify fluxes of nutrients and carbon in the ocean at regional and basin scales (Orr and Sarmiento, 1992; Sarmiento *et al.*, 1993; Fasham *et al.*, 1993; Fasham, 1995; McCreary *et al.*, 1996; Oschlies and Garçon, 1998, 1999). In most implementations, the coupling of physical and biological models presupposes relatively simple biological equations that are general and robust across seasons and biogeographical regimes (Fasham *et al.*, 1993). Most commonly used biogeochemical models adopt nitrogen or phosphorus as a natural "currency" under the assumption that NO_3 or PO_4 is the limiting nutrient in marine systems. Model compartments are then expressed as equivalent scalar concentrations of nitrogen (Fasham *et al.*, 1990) or phosphorus (Doveri *et al.*, 1993) (But note recent work on other limiting nutrients such as iron; Moore *et al.*, 2000). These models are based on a pragmatic approach to the functional categorization of organisms and largely ignore taxonomic hierarchies and food web complexities common to such systems (Pomeroy, 1974). Nevertheless, this class of models provides a useful and relatively simple general framework to describe and analyze ecosystem functioning. In addition, the use of bulk variables facilitates the evaluation of such models against in-situ chlorophyll and primary productivity measurements as well as satellite data. The overall test of these models is whether they skillfully

reproduce field observations, challenge conventional wisdom and create new hypotheses.

Although these food web models are being widely used in combination with general circulation models, relatively little work has been done on understanding their intrinsic dynamics independently of physical forcing (e.g., Busenberg *et al.*, 1990; Doveri *et al.*, 1993; Edwards and Brindley, 1996)). Due to their nonlinear nature, these models can display a wide range of dynamical behaviors. Asymptotically stable equilibrium points transition to limit cycles and to chaotic oscillations as parameters or forcing variables are changed (Hastings and Powell, 1991; Ascioti *et al.*, 1993; Doveri *et al.*, 1993; McCann and Yodzis, 1994; Edwards and Brindley, 1996; Edwards *et al.*, 2000). These qualitative changes in the model dynamics have important implications for the interpretation and fit to observations of coupled physical-biological models. Because phytoplankton growth rates depend on light and nutrients, model dynamics should be expected to vary seasonally, geographically and with depth, even in the absence of physical processes (e.g., advection and diffusion). In more complex biogeochemical models, with a higher number of species or functional groups, this temporal and spatial variation in model dynamics, combined with advection and diffusion, will also have important consequences for species persistence/coexistence and pelagic biogeography (Olson and Hood, 1994).

In this study, the intrinsic dynamics of three common formulations for the NPZD class of models using two different types of predation functional response are analyzed and compared. Our goal is to characterize the changes in the dynamical behavior of this class of models with respect to variations in light and total nutrient concentrations. The results are discussed in terms of model stability and its implications for species persistence/coexistence and the dynamics of the chlorophyll maximum layer. A basic understanding of the steady state intrinsic dynamics of this class of biological models is a necessary first step in the study of the impact of physical processes and variability on biological production in the oceans using coupled physical-biogeochemical models and the development of more realistic and robust ecosystem models.

Methods

General Model Form

Currently, many large-scale coupled physical-biological models are based on comparatively simple trophic interaction models with few basic compartments, nutrients, phytoplankton, zooplankton and detritus (so called NPZD class of models) (Fasham *et al.*, 1990; Eslinger, 1990; Sarmiento *et al.*, 1993; Fasham *et al.*, 1993; Doney *et al.*, 1996). Because plankton communities are composed of many taxonomically and biogeochemically distinct species with a wide range of size classes, this model form is often adapted by including more than one compartment at each trophic level and incorporating size structure (Banse, 1994).

The three model formulations analyzed are part of this NPZD class of models in which model compartments are expressed as their equivalent scalar concentrations of nitrogen. The structural relationship among the different compartments in each model is outlined in Figure 1. The model series starts with the simplest case of a single species or size class in each trophic level (NPZD) and then successively adds one size class for the phytoplankton (NPPZD) and then for both phytoplankton and zooplankton (NPPZZD). The general form of the time rate of change equations are:

$$\dot{P}_i = U_i(I,N)\,P_i - g_i\,G_i(P_i)\,Z_i - s_i\,P_i \tag{1}$$

$$\dot{Z}_i = a_i\,m_i\,g_i\,G_i(P_i,Z_j,D)\,Z_i - d_i\,Z_i^2 \tag{2}$$

$$\dot{D} = \sum_i \left((1-a_i)\,g_i\,G_i(P_i,Z_j,D)\,Z_i - g_i\,G_i(D)\,Z_i + s_i\,P_i + d_i\,Z_i^2\right) - e\,D \tag{3}$$

$$\dot{N} = \sum_i \left(a_i\,(1-m_i)\,g_i\,G_i(P_i,Z_j,D)\,Z_i - U_i(I,N)\,P_i\right) + eD \tag{4}$$

$$N_0 = N + D + \sum_i P_i + \sum_i Z_i \tag{5}$$

for $i = 1, 2$ refering to the number of species or size classes (small and large, respectively) in the phytoplankton and zooplankton compartments. In the zooplankton compartment, Z_j refers to zooplankton species or size class $i-1$, when $i = 2$. N_0 is the total amount of nitrogen in the system, and the dot ($\dot{}$) denotes the time derivative.

[Figure 1 about here.]

Phytoplankton growth is controlled by light (I) and nutrient concentration (N) and losses through grazing and senescence (mortality). The relationship between photosynthesis and light is given by a standard exponential $P-I$ curve (Cullen, 1990):

$$P_B = P_{B_{max}}\left(1 - e^{-\alpha I_{par}/P_{B_{max}}}\right) \tag{6}$$

where P_B (mMol N (mg Chl^{-1}) day^{-1}) is the assimilation rate of N normalized to chlorophyll, $P_{B_{max}}$ is the maximum assimilation rate, α is the initial slope of the curve, and I_{par} is the photosynthetically available radiation (PAR). The use of a single $P-I$ curve is acceptable if we assume that the phytoplankton are adapted to the irradiance level at which they are growing (Cullen, 1990). The assimilation rate can be converted into specific growth rates u (day^{-1}) by multiplying it by the chlorophyll/nitrogen ratio $[chl:N]$ (mg Chl (mMol N)$^{-1}$), which is assumed to be constant:

$$u = [chl:N]\,P_B\,; \quad u_{max} = [chl:N]\,P_{B_{max}} \tag{7}$$

Substituting (7) into (6) and adding the effect of nutrients in the form of a Michaelis-Menten term we arrive at a phytoplankton growth function of the form:

$$U(I_{par}, N) = u_{max}\left(1 - e^{-\alpha I_{par}[chl:N]/u_{max}}\right)\left(\frac{N}{K_P + N}\right) \tag{8}$$

where K_P is the nutrient half saturation concentration.

The light intensity available for photosynthesis (I_{par}) at depth (z) is given by:

$$I_{par} = I_0\,\theta\,e^{-\lambda z} \tag{9}$$

where I_0 is the total irradiance at the surface, θ is the fraction of total irradiance that is available for photosynthesis (PAR) and λ is the light attenuation coefficient. The diurnal cycle of light intensity is ignored, and I_0 is set to the annual mean for 30^o N (List, 1971). The reader should note that one could add explicit wavelength dependence and phytoplankton self-shading to the model formulation. While those are important for simulationg specific conditions, they do not change the conclusions here and therefore, are not considered.

Zooplankton growth is a function of total food availability ($G_i(P_i, Z_j, D)$) - phytoplankton, detritus and, in the NPPZZD model, zooplankton. In the multi-species cases (NPPZD and NPPZZD), zooplankton feeds on phytoplankton of the same size index i. Two different forms of zooplankton predation functional response, based on the Michaelis-Menten equation, are used in each of the three model formulations. The first form (fixed preferences) is given by:

$$G(S) = \frac{\sum \phi_{S_n} S_n}{K_Z + \sum \phi_{F_n} F_n} \tag{10}$$

where S_n represent the food sources being consumed and F_n represent all the different food sources available (including S), ϕ_{F_n} is the preference for food source F_n when all food sources have equal concentration, and

K_Z is the half-saturation constant for zooplankton grazing. Here a common index convention is being used when the sum is over all *i* components. For example:

$$G(P) = \frac{\phi_P P}{K_Z + (\phi_P P + \phi_Z Z + \phi_D D)} \; ; \quad G(P,Z,D) = \frac{\phi_P P + \phi_Z Z + \phi_D D}{K_Z + (\phi_P P + \phi_Z Z + \phi_D D)}$$

In the second form of predation functional response, the preference terms for the different food sources change as a function of the relative proportion of the available food. This change is implemented by defining weighted preferences (ϕ'_n) as in Fasham *et al.* (1990):

$$\phi'_n = \frac{\phi_n S_n}{\sum_j \phi_n S_n} \tag{11}$$

Thus, for example, the preference of large zooplankton for large phytoplankton is defined as:

$$\phi'_{P_2} = \frac{\phi_{P_2} P_2}{\phi_{P_2} P_2 + \phi_{Z_1} Z_1 + \phi_D D} \tag{12}$$

where ϕ_{P_2}, ϕ_{Z_1} and ϕ_D are the nominal preferences for large phytoplankton, small zooplankton and detritus when these food sources have equal concentration. The use of weighted preferences is equivalent to the "distributed grazing model" of Armstrong (1999), in which the zooplankton compartment is assumed to represent a diverse grazing community, and can actively select the most abundant food item (see Appendix A in Fasham *et al.*, 1990). Substituting the expression for the weighted preferences (ϕ'_n) for the ϕ_n values in Equation 10 we obtain predation functional responses for the zooplankton ($\hat{G}$) of the form:

NPZD model:

$$\hat{G}(P,D) = \frac{\phi_P P^2 + \phi_D D^2}{K_Z (\phi_P P + \phi_D D) + (\phi_P P^2 + \phi_D D^2)} \tag{13}$$

NPPZD model:

$$\hat{G}(P_1, P_2, D) = \frac{\phi_{P_1} P_1^2 + \phi_{P_2} P_2^2 + \phi_D D^2}{K_Z (\phi_{P_1} P_1 + \phi_{P_2} P_2 + \phi_D D) + (\phi_{P_1} P_1^2 + \phi_{P_2} P_2^2 + \phi_D D^2)} \tag{14}$$

NPPZZD model:

$$\hat{G}_1(P_1, D) = \frac{\phi_{P_1} P_1^2 + \phi_D D^2}{K_{Z_1} (\phi_{P_1} P_1 + \phi_D D) + (\phi_{P_1} P_1^2 + \phi_D D^2)} \tag{15}$$

$$\hat{G}_2(P_2, Z_1, D) = \frac{\phi_{P_2} P_2^2 + \phi_{Z_1} Z_1^2 + \phi_D D^2}{K_{Z_2} (\phi_{P_2} P_2 + \phi_{Z_1} Z_1 + \phi_D D) + (\phi_{P_2} P_2^2 + \phi_{Z_1} Z_1^2 + \phi_D D^2)} \tag{16}$$

All losses in the zooplankton compartments occur through predation by a higher trophic level. This is represented by the nonlinear term $-d_i Z_i^2$, which implies that the predator biomass increases in proportion to the zooplankton abundance. A quadratic closure was chosen because it stabilizes the model at extreme zooplankton concentrations (Steele and Henderson, 1992; McCreary *et al.*, 1996).

The contribution of fecal pellets (produced by grazing) to the detritus compartment is represented in the model by the parameterization of assimilation efficiencies (a_i). Other sources of detritus are phytoplankton senescence ($s_i P_i$) and zooplankton mortality ($d_i Z_i^2$). Losses in this compartment occur through remineralization ($e D$) and consumption by zooplankton.

The dissolved nutrient compartment receives input from remineralization of detritus and excretion proportional to zooplankton grazing. The latter process is parameterized in the model in terms of metabolic efficiencies (m_i). Losses occur through uptake by the phytoplankton. Bacterial activity is included implicitly by assuming a rapid transformation of dissolved organic nitrogen into inorganic nitrogen (the nutrient pool includes NO_3, NO_2, NH_3 and labile dissolved organic nitrogen, DON) and in the parameterization of the remineralization of detrital material. The "microbial loop" (DON - bacteria - microzooplankton) is also represented implicitly by including bacteria in the detritus compartment and parameterizing the consumption

of some detritus by the zooplankton.

Model Parameterization

The three biological models were parameterized to represent the plankton communities in subtropical oligotrophic oceans. The parameter values and definitions for the general single-species (NPZD) model are given in Table I. Estimates for phytoplankton maximum growth rates (u_{max}) in warm subtropical waters vary between 1.5 and 3.0 day^{-1} (Eppley, 1972, 1980; Prezelin *et al.*, 1991; Fasham *et al.*, 1990; McCreary *et al.*, 1996; Geider *et al.*, 1997) and a value of 2.0 day^{-1} is chosen. K_P and K_Z are generally low for oligotrophic phytoplankton and zooplankton and are set to 0.6 and 1.0 mMol N m^{-3} respectively (Eppley *et al.*, 1969; Parsons *et al.*, 1984). Measurements of α range from 0.01 to 0.08 mMol N (mg Chl)$^{-1}$ day^{-1} m^2 W^{-1} (Platt *et al.*, 1983; Peterson *et al.*, 1987; Platt *et al.*, 1992; Cullen *et al.*, 1992) (converted using $C:N=6.6$), and a value of 0.025 is used. The photosynthetically available radiation (PAR) corresponds to 0.40 to 0.50 of the total incoming radiation at the surface (Parsons *et al.*, 1984; Kirk, 1992), and a constant value of 0.45 is used in the model. The light attenuation coefficient is set to 0.035 m^{-1} (Parsons *et al.*, 1984). There are very few observational data on the phytoplankton natural mortality rate (s) (e.g., Brussaard *et al.*, 1995)) so its value is chosen (0.01 day^{-1}) to give a reasonable phytoplankton biomass and to be consistent with previous studies (Franks *et al.*, 1986; Wroblewski, 1989; Fasham *et al.*, 1990). The $[chl:N]$ ratio is taken as 1.0 mg Chl (mMol N)$^{-1}$ (Marra *et al.*, 1990). Zooplankton growth rates (g) range from 0.5 to 2.0 day^{-1} (Evans and Parslow, 1985; Franks *et al.*, 1986; Hansen *et al.*, 1997) and a value of 1.0 day^{-1} is used. In the model, zooplankton consume phytoplankton and detritus. The food source preference terms are chosen to represent a predominantly herbivorous zooplankton community. Assimilation efficiencies for zooplankton vary from 0.1 to 0.8 (Evans and Parslow, 1985; Fasham *et al.*, 1990; McCreary *et al.*, 1996). The somewhat high value of 0.8 is used to account for the higher assimilation efficiencies of the microzooplankton, which tend to be

more dominant in oligotrophic environments (Sorokin, 1981; Sieburth, 1982; Azam *et al.*, 1994). Zooplankton excretion accounts for 50 to 95 % of the nitrogen recycled in the euphotic zone in marine oligotrophic environments (Eppley and Peterson, 1979; Harrison, 1980; Bidigare, 1983; Harrison, 1992) To achieve high excretion rates, a relatively low metabolic efficiency (m) of 0.25 is used in the model. This choice results in an overall growth efficiency of 0.2, which is within the range of values reported for zooplankton (Parsons *et al.*, 1984; Banse, 1994). Oligotrophic oceans are characterized by effective nutrient recycling (Eppley and Peterson, 1979; Harrison, 1980; McCarthy and Carpenter, 1983; Harrison, 1992), and a value of 0.25 day^{-1} (Harrison, 1980) is used for the detritus remineralization rate.

[Table 1 about here.]

The parameter values used in the NPPZD and NPPZZD models (Table II and III) were obtained from the same range of reported estimates used for the single-species (NPZD) model. However, parameter values were chosen to reflect the size-related differences in growth and mortality rates and metabolic efficiencies. The smaller phytoplankton and zooplankton size classes have higher growth and mortality rates and metabolic efficiencies and lower half saturation constants in the nutrient uptake and grazing terms. The parameter values used in this study are well within the range of values used in most biogeochemical modeling studies (e.g., Fasham *et al.*, 1990; Moloney and Field, 1991; Doney *et al.*, 1996; McGillicuddy *et al.*, 1998; Oschlies and Garçon, 1998)).

[Table 2 about here.]

[Table 3 about here.]

Experiments and Analysis

The steady-state dynamics of the biological models were investigated with respect to variations in light and the total amount of nitrogen, which are the primary factors controlling the biological systems. Because of the nonlinear nature of the functional responses and closure terms for zooplankton, it is quite difficult to compute solutions for the equilibrium points of the biological equations analytically. Thus, the computation of equilibrium points and subsequent analysis of stability were done numerically. The numerics have been checked against simplified models that allow analytical computation of fixed points (Olson *et al.*, 2001). The biological model equations were integrated using the 4^{th} order Runge-Kutta method.

Results

NPZD Model

Fixed Preferences

As expected, equilibrium values of P, Z and D increase with total nitrogen and light (Figure 2) while N increases with N_0 and as light decreases. However, the increase in N equilibrium values along the N_0 direction is not monotonic (Figure 2c). For values of N_0 above 2.25 mMol N m^{-3}, there is a range of light intensities (I_{par}) where the system becomes unstable (shaded gray area in Figure 2). In this area, N, P, Z and D are nonzero and positive but oscillate in a limit cycle (Figure 3a). The variation in model equilibrium values as a function of light (I_{par}) are shown in Figure 4 for fixed amounts of total nitrogen ($N_0 = 2.0$ and $N_0 = 9$ mMol N m^{-3}). At moderate total nitrogen concentrations (Figure 4a), the system has one non-trivial equilibrium state ($N > 0$, $P > 0$, $Z > 0$, $D > 0$). P, Z and D concentrations decrease and N increases as light intensity decreases. Below $I_{par} \approx 1$ W m^{-2}, P, Z and D become extinct, and all the nitrogen in the system is

in the N compartment ($P = Z = D = 0$ and $N = N_0$). No limit cycles or orbits are observed and the single-species model is stable over all the range of I_{par} values. For $N_0 = 9$ mMol N m^{-3}, P, Z and D equilibrium concentrations also decrease with light while N increases. However, for light intensities between 7 and 17 W m^{-2} the system becomes unstable (Figure 4b). At this range of light intensities, which correspond to depths between 59 and 85 m, the nonzero equilibrium point loses its stability, and a periodic orbit is formed through a Hopf bifurcation. The Hopf bifurcation involves the creation or destruction of a periodic orbit through a change in the stability of an equillibrium point (Hale and Koçak, 1991). As light levels drop below 7 W m^{-2} (depth $>$ 85 m) the periodic orbit collapses back into a nonzero asymptotically stable equilibrium point. And finally, when I_{par} again reaches $\approx$ 1 W m^{-2} (depth $\approx$ 140 m), P, Z and D become extinct, and all the nitrogen in the system is in the N compartment (Figure 4b).

[Figure 2 about here.]

[Figure 3 about here.]

[Figure 4 about here.]

Although the model is structurally stable for $N_0 < 2.25$ mMol N m^{-3}, the time it takes to reach equilibrium values increases significantly as light decreases with depth (Figure 5). Transient times are of the order of 40 days for depths above 25 m (Figures 5a), 90 days at 50 m and several hundred days, i.e. seasonal time scales, for depths below 75 m (Figures 5c,d). Transient times at a given depth (light intensity) also become gradually longer as N_0 increases, denoting the transition from a stable equilibrium to a limit cycle at depths below 59 m. For high nutrient states, $N_0 > 2.25$ mMol N m^{-3}, transient times are infinite at depths between 59 and 85 m, and the system oscillates in a periodic orbit (Figure 3a). Variation in the transient times with depth will have important consequences for the dynamics of the biological model in the presence of physical perturbations.

[Figure 5 about here.]

Variable Preferences

The use of weighted preferences (Equation 11) in the predation functional response increases the stability of the model significantly. Limit cycle oscillations start at a higher value of total nitrogen ($N_0 > 3.3$ mMol N m^{-3}) and occur at a narrower range of light intensities (Figure 6). For example, for $N_0 = 9$ mMol N m^{-3}, the model is unstable for I_{par} between 12 and 18 W m^{-2}, which correspond to depths between 58 and 69 m (Figure 7b). Variable preferences in the functional response result in slightly lower P and higher D equilibrium concentrations than in the previous case, as Z is able to switch to the most abundant food item (Figure 7a).

[Figure 6 about here.]

[Figure 7 about here.]

Transient times are also shorter when variable preferences are used. At 25 m, transient times are of the order of 30 days, 75 days at 50 m (Figure 8a,b). Below 75 m, transient times are of the order of several hundred days. As in the model with fixed preferences, transient times at a given depth (light intensity) also become gradually longer as N_0 increases (not shown).

[Figure 8 about here.]

NPPZD Model

Fixed Preferences

In the NPPZD model, limit cycle oscillations are also present at low I_{par} and moderate to high N_0 (Figure 9). For the range of parameter values used in this study (Table II), there is also competitive exclusion of species.

With fixed preferences in the predation functional response, the inclusion of a faster growing phytoplankton species (P_1) results in the extinction of the slower growing species (P_2).

[Figure 9 about here.]

The transition between the different equilibria as light (I_{par}) varies but for fixed amounts of total nitrogen (N_0) is shown in Figure 10. For $N_0 = 2.5$ mMol N m^{-3} (Figure 10a), the system has one non-trivial asymptotically stable equilibrium state at $I_{par} > 0.4$ W m^{-2} (depth < 160 m), where all compartments, except P_2, are nonzero and positive ($N > 0$, $P_1 > 0$, $P_2 = 0$, $Z > 0$, $D > 0$). As I_{par} drops below 0.4 W m^{-2}, P_1, Z and D become extinct and all nitrogen is in the N compartment ($P_1 = P_2 = Z = D = 0$ and $N = N_0$). For $N_0 = 9$ mMol N m^{-3} (Figure 10b), the system has an asymptotically stable equilibrium point ($N > 0$, $P_1 > 0$, $P_2 = 0$, $Z > 0$, $D > 0$) for $I_{par} > 6.8$ W m^{-2} (depth < 85 m) and a periodic orbit for I_{par} between 6.8 and 4 W m^{-2}. At $I_{par} \approx 4$ W m^{-2} (depth ≈ 101 m), the orbit collapses into another asymptotically stable equilibrium point ($N > 0$, $P_1 > 0$, $P_2 = 0$, $Z > 0$, $D > 0$). Finally, as I_{par} drops below 0.4 W m^{-2} (depth > 166 m) P_1, Z and D become extinct and all the nitrogen in the system is in the N compartment ($P_1 = P_2 = Z = D = 0$ and $N = N_0$).

[Figure 10 about here.]

Within the stable range of N_0 values ($N_0 < 7.8$ mMol N m^{-3}), the time it takes the system to reach equilibrium is also considerably longer than in the previous NPZD formulation. Transient times are of the order of 300 days at depths lower that 25 m and several hundred days below 50 m (not shown).

Variable Preferences

As in the previous NPZD model formulation, the use of variable preferences increases the overall stability of the system (Figure 11). However, a small unstable area is still observed at $N_0 > 5.3$ mMol N m^{-3} and low

light intensities. For $N_0 > 5.3$ mMol N m^{-3}, the system oscillates in a limit cycle for I_{par} values between 6.3 and 8.3 W m^{-2} (depths between 80 and 88 m) (Figure 12b). For $N_0 < 5.3$ mMol N m^{-3}, no oscillations or limit cycles are observed (Figure 12a). The use of variable preferences also makes it possible for P_1 and P_2 to coexist over most of the parameter space ($N_0 > 0$ mMol N m^{-3} and $I_{par} > 0.4$ W m^{-2}).

[Figure 11 about here.]

[Figure 12 about here.]

The time the system takes to reach equilibrium is considerably shorter than in the formulation with fixed preferences but still longer than in the previous NPZD model with variable preferences. Transient times are of the order of 50 days at depths lower than 50 m, 150 days at 75 m, and several hundred days at 100 m (not shown).

NPPZZD Model

Fixed Preferences

For the range of parameter values used in this modeling study (Table III), the addition of another zooplankton species or size class to the previous NPPZD model, with fixed preferences in the predation functional response, results in an unrealistically unstable model. There are limit cycles of various periods and several different equilibrium states with one or more compartments extinct (not shown). Competitive exclusion of species is also observed over large areas of the parameter space. Preliminary experiments show that in order to achieve some degree of stability and species coexistence with this model formulation, the parameter values would have to be significantly different from those shown in Tables I, II and III. That, however, would undermine the comparison of results from the different models formulations. Because of its varied behavior, the detailed analysis of the dynamics of this model formulation is beyond the scope of this study.

Variable Preferences

The use of variable preferences results in a significantly stabler model. Although the equilibrium concentration of P_1 and P_2 tend to be inversely correlated, the different species of phytoplankton and zooplankton are able to coexist over most of the parameter space (Figure 13). For $N_0 > 4$ mMol N m^{-3} and light intensities approximately between 5 and 12 W m^{-2} (depths between 94 and 69 m), the system becomes unstable and P_1, P_2, Z_1, Z_2, N and D equilibrium values oscillate in a limit cycle (shaded gray area in Figure 13).

[Figure 13 about here.]

For a fixed amount of total nitrogen (N_0), the position of P_1, P_2, Z_1, Z_2, N and D equilibrium values as light varies is shown in Figure 14. For $N_0 = 2.5$ mMol N m^{-3}, the system has one non-trivial equilibrium state ($N > 0$, $P_1 > 0$, $P_2 > 0$, $Z_1 > 0$, $Z_2 > 0$, $D > 0$) for $I_{par} > 0.4$ W m^{-2} (Figure 14a). As I_{par} drops below 0.4 W m^{-2} (depth $>$ 166 m), P_1, P_2, Z_1, Z_2, and D become extinct and all the nitrogen in the system is in the N compartment. For $N_0 = 9$ mMol N m^{-3}, P_2 (Figure 14b), the system has an asymptotically stable equilibrium point ($N > 0$, $P_1 > 0$, $P_2 > 0$, $Z_1 > 0$, $Z_2 > 0$, $D > 0$) for $I_{par} > 12$ W m^{-2} (depth $<$ 69 m) and a periodic orbit for I_{par} between 6 and 12 W m^{-2}. In the unstable region, the range of variation of P_1 and Z_1 is much greater than that of P_2 and Z_2. At I_{par} below 6 W m^{-2} (depth $>$ 89 m), the periodic orbit collapses back into an nonzero asymptotically stable equilibrium point, and when I_{par} reaches approximately 0.4 W m^{-2} (depth $\approx$ 166 m), P_1, P_2, Z_1, Z_2 and D become extinct and all the nitrogen in the system is in the N compartment.

[Figure 14 about here.]

Within the stable range of parameters ($N_0 < 4$ mMol N m^{-3}), transient times in the multi-species model (Figure 15) are significantly longer compared to those in the NPZD and NPPZD models with variable

preferences (Figure 8). Transient times are of the order of 300 days for depths above 75 m and several hundred days below 100 m (Figure 15). However, total phytoplankton ($P_1 + P_2$) and zooplankton ($Z_1 + Z_2$) reach relatively constant concentrations in considerably less time (Figure 16). Transient times for total phytoplankton and zooplankton are of the order of 150 days at depths above 50 m, 200 days at 75 m but still several hundred days at 100 m and below (Figure 16).

[Figure 15 about here.]

[Figure 16 about here.]

Discussion

Despite important structural differences, the various model formulations have similar dynamical responses to variations in light intensity and total nutrient concentration. All models have asymptotically stable equilibrium points at low total nitrogen concentrations and high to moderate light intensities, and oscillate in a limit cycle at low light intensities and moderate to high total nitrogen concentrations. The potential for phytoplankton–zooplankton systems to display oscillatory behavior has been demonstrated in field studies (McCauley and Murdoch, 1987; Williams, 1988; Ascioti *et al.*, 1993) as well as in laboratory experiments (Goulden and Hornig, 1980). Oscillations in chlorophyll concentrations have been observed at Ocean Weather Station (OWS) I (Williams, 1988) and P (Figures 1 and 2 in Ryabchenko *et al.*, 1997) associated with high nitrogen concentrations in the pycnocline. In Bermuda, where surface conditions are oligotrophic throughout most of the year, oscillations in chlorophyll concentrations have not been observed. At depth near the nutricline, however, oscillations might be present but may not be captured by sampling due to the temporal resolution of the observations and the added variablility driven by physical processes such as mesoscale eddies and turbulent mixing events. The tendency of structured predator-prey models to become

unstable with enrichment has also been documented by Rosenzeig (1971). These observations are consistent with the dynamical behavior of the models described in this study. However, the oscillations observed at OWS I and P have a period of the order of 40 days (Williams, 1988; Ryabchenko *et al.*, 1997), whereas in the models the period of the oscillations ranges from 50 to 100 days, with the multi-species formulations having the longest period.

As the number of compartments or species increases, the models tend to become unstable over a progressively wider range of light intensities and total nitrogen concentrations. This is expected as the tendency for instabilities increases with the dimensionality of the system (Schaffer, 1985; Hale and Koçak, 1991). The longer transient times seen in the multi-species formulations (NPPZD and NPPZZD) are directly related to their reduced stability. More parts interacting lead to more complex dynamics and therefore to longer transient times. In the NPZD (single-species) model, the sequence of events starting from high concentrations of N and low concentrations of P, Z, and D is: $P\uparrow \Rightarrow N\downarrow \Rightarrow Z\uparrow \Rightarrow P\downarrow$ (upward and downward arrows denote increases and decreases in the components involved, respectively) (Figure 5). P grows, consuming N and declines in reponse to intensified grazing by Z. In the NPPZZD model (with variable preferences) the sequence is as follows: $P_1\uparrow \Rightarrow Z_1\uparrow \Rightarrow P_1\downarrow \Rightarrow P_2\uparrow \Rightarrow Z_2\uparrow \Rightarrow P_2\downarrow \Rightarrow P_1\uparrow$ (Figure 15). P_1 responds first to the higher N concentrations because of its higher growth rate and lower half saturation constant, and declines as grazing by Z_1 intensifies. P_2 increases in respose to the reduced competition for nutrients and subsequently declines under increased grazing by Z_2. As Z_2 grows, P_2 and Z_1 concentrations decline due to grazing and P_1 starts to grow again, in response to the reduced competition for N and lower grazing by Z_1. The sequence of events for total phytoplankton and zooplankton, however, is very similar to that of the single-species model ($P_{tot}\uparrow \Rightarrow N\downarrow \Rightarrow Z_{tot}\uparrow \Rightarrow P_{tot}\downarrow$), and total phytoplankton and zooplankton reach equilibrium concentrations significantly sooner than its individual constituents (Figure 16). Thus, although the individual compartments or species tend to oscillate in time, the functional groups (total phytoplankton

and total zooplankton) and overall multi-species system can remain relatively stable (Figure 16).

The form of the predation functional response has an important effect on the overall stability of the systems. The use of variable preferences in the functional response is equivalent to assuming that the zooplankton compartment represents a diverse community of grazers and, therefore, is able to actively select the most abundant food item (Fasham *et al.*, 1990; Armstrong, 1994, 1999). This "distributed grazing model" (Armstrong, 1999) is analogous to a Holling type III functional response for multiple prey items (Case, 2000). The "predator switching" mechanism, characteristic of this type of functional response, provides a density-dependent mechanism that dampens oscillations by increasing the loss rate of the prey species or compartments that are temporarily more abundant, increasing system stability considerably. The presence of density-dependent mechanisms is particularly important in multi-species formulations which are more prone to predator-prey oscillations and competitive exclusion of species (Schaffer, 1985; Hale and Koçak, 1991). The change in behavior (stability properties and ability of species to coexist) resulting from the type of preference used in the functional response is most marked in the NPPZD and NPPZZD models. In the NPPZZD model, the use of fixed preferences results in an unrealistically unstable model. The multi-species models (NPPZD and NPPZZD) also illustrate the importance of grazing for the coexistence of phytoplankton species that depend on a single nutrient resource. In addition to stabilizing oscillations, the "predator switching" mechanism provided by the variable preferences counteracts the tendency for competitive exclusion of species by reducing the loss rate of the rarer of several competing species (Roughgarden and Feldman, 1975).

However, despite the use of a density-dependent grazing formulation, instabilities are still observed at low light and high total nitrogen concentrations, in all models. A stable limit cycle is formed in all models as the asymptotically stable equilibrium point undergoes a Hopf bifurcation. The Hopf bifurcation involves a split in the solution into a periodic orbit around the equilibrium point (which becomes unstable), as a phase

lag occurs between predator (Z_i) and prey (P_i or Z_{i-1}). In the NPZD and NPPZD models, the phase lag is caused by a increase in the growth rate of the phytoplankton (P_i) in relation to that of the zooplankton, as equilibrium nutrient concentrations increase at low light levels (Figure 17a,b). The zooplankton is no longer able to track the growth in phytoplankton abundance and the system starts to oscillate in a limit cycle. In the NPPZZD model, the phase lag is a result of the sharp drop in the ratio between Z_2 and P_2 and, Z_2 and Z_1 growth rates (Figure 17c).

[Figure 17 about here.]

In most ocean environments, light intensity decays exponentially with depth while, N_0 increases with depth. The range of values of light intensity and total nitrogen for which the different models are unstable correspond to those observed on the bottom of the euphotic zone near the nutricline, where the deep chlorophyll maximum is usually located. This suggests that the deep chlorophyll maximum might be dynamically unstable, with the abundance of the different phytoplankton species oscillating in time. This dynamical disequilibrium in species composition would provide a mechanism for species coexistence in the relatively homogeneous open ocean environment. This last problem is referred to as the "paradox of plankton" (Hutchinson, 1961). The combination of physical perturbations (e.g., intermittent or seasonal mixing events) and the characteristically long transient times at low light and high total nitrogen concentrations, would also favor species coexistence and allow persistence of species at seasonal to annual time scales. Studies in the central North Pacific show high species diversity ($>$ 300 phytoplankton species) but no evidence of niche partitioning or microhabitat formation (Venrick, 1986, 1988). In addition to high species diversity, Venrick (1990) also reported a slow but significant nondirectional change in the structure of the deep phytoplankton community (deep chlorophyll maximum) of the central North Pacific over time scales consistent with the transient times at the corresponding depths in the multi-species model (several hundred

days) (Figure 15).

The changes in the model dynamics with light and total nutrient are particularly relevant to biogeochemical calculations using coupled physical-biological models. The distinct dynamical regimes in the upper and lower part of the euphotic zone can interact with advection and vertical mixing to produce complex temporal and spatial patterns of plankton distribution (Okubo, 1978; Levin, 1978). The shifts in model dynamics associated with seasonal and geographical variations in light intensity and nutrients, in combination with advection and the characteristically long transient times will also affect large scale temporal and spatial patterns of plankton distribution and pelagic biogeography (Olson and Hood, 1994).

The higher diversity of species in the NPPZD and NPPZZD models (wider range of values for the biological parameters , Tables II and III), allows biological activity (photosynthesis, grazing and predation) to occur under a wider range of light and nutrient conditions (Figure 18). Recycling through zooplankton excretion and consumption of detritus is also enhanced in the NPPZZD model. As a result, primary and secondary production are higher in the multi-species models (Figure 18a and b). The higher biological production integrated over the whole range of light intensities in the multi-species models result in more nitrogen in the biotic compartments and, therefore, in a more oligotrophic environment (low N) at light intensities equivalent to those in the upper part of the euphotic zone (Figure 18c).

[Figure 18 about here.]

Concluding Remarks

Plankton communities are composed of a diverse mixture of taxonomically and biogeochemically distinct groups. However, computational costs and the difficulty in parameterizing complex food webs impose severe limits on the construction/formulation of realistic ecosystem models. Thus, current ecosystem models

are based on deterministic predator-prey models with a relatively small number of highly aggregated compartments, in which biological fluxes are formulated in terms of a common chemical "currency". In this study we show that commonly used biogeochemical formulations are dynamically unstable at levels of total nitrogen and light intensity that correspond to those observed at the base of the euphotic zone near the nutricline, where the deep chlorophyll maximum is usually located. The inclusion of density-dependent regulatory mechanisms, such as variable variable preferences in the predation functional response (Fasham *et al.*, 1990; Armstrong, 1999), reduce the range of light intensities and total nitrogen values for which the models are unstable significantly, but do not eliminate the unstable regions. The existence of instabilities at low light and high nutrient concentrations could have important consequences/implications for the dynamics of deep chlorophyll maximum and the maintenance of high species diversity in relatively homogeneous oceanic environment.

The presence of physically generated noise (mixing advection and mesoscale turbulence) could change the aforementioned results considerably. The effects of stochastic perturbations and mixing are often diverse and sometimes non-intuitive. Noise can substantially modify the base state and stability of deterministic ecosystem models (May, 1973), and the addition of dynamic noise or diffusion can destabilize an otherwise stable system, or vice-versa (Crutchfield *et al.*, 1982; Rand and Wilson, 1991; Pascual, 1993; Edwards *et al.*, 2000). The role of stochasticity in the dynamics of aquatic ecosystem models is the subject of a forthcoming paper.

Acknowledgments

The authors would like to thank the anonymous reviewers for their relevant comments and suggestions. Support for this work was provided by the *Conselho Nacional de Desenvolvimento Científico e Tecnológico*

(CNPq, Brazil), Office of Naval Research Grant #N00014-96-10421 and the NASA SeaWiFS Grant W-19,223. The National Center for Atmospheric Research is sponsored by the National Science Foundation.

References

Armstrong, R. A. (1994) Grazing limitation and nutrient limitation in marine ecosystems: steady state solutions of an ecosystem model with multiple food chains. *Limnol. Oceanogr.*, **39**(3), 597–608.

Armstrong, R. A. (1999) Stable model structures for representing biogeochemical diversity and size spectra in plankton communities. *J. Plankton Res.*, **21**(3), 445–464.

Ascioti, F. A., Beltrami, E., Carroll, T. O. and Wirick, C. (1993) Is there chaos in plankton dynamics? *J. Plankton Res.*, **15**(6), 603–717.

Azam, F., Fenchel, T., Field, J. G., Gray, J. S., Meyer-Reil, L. A. and Thingstad, F. (1994) The ecological role of water-column microbes in the sea. *Mar. Ecol. Prog. Ser.*, **10**, 257–263.

Banse, K. (1994) Grazing and zooplankton production as key controls of phytoplankton production in the open ocean. *Oceanography*, **7**(1), 13–20.

Bidigare, R. R. (1983) Nitrogen excretion by marine zooplankton. In Carpenter, E. J. and Capone, D. G. (eds.), *Nitrogen in The Marine Environment*, Academic Press, New York, pp. 385–409.

Brussaard, C. P. D., Riegman, R., Noordellos, A. A. M., Cadee, G. C., Witte, H., Kop, A. J., Nieuwland, G., van Duyl, F. C. and Bak, R. P. (1995) Effects of grazing, sedimentation and phytoplankton cell lysis on the structure of a coastal pelagic food web. *Mar. Ecol. Prog. Ser.*, **123**, 259–271.

Busenberg, S., Kumar, S. K., Austin, P. and Wake, G. (1990) The dynamics of a plankton-nutrient interaction. *Bull. Math. Biol.*, **52**(5), 677–697.

Case, T. J. (2000) *An Illustrated Guide to Theoretical Ecology*. Oxford University Press, Oxford.

Crutchfield, J., Farmer, J. and Huberman, B. A. (1982) Fluctuations and simple chaotic dynamics. *Phys. Rep.*, **92**, 45–82.

Cullen, J., Yang, X. and MacIntyre, L. (1992) Nutrient limitation and marine photosynthesis. In Falkowski, P. G. and Woodhead, A. D. (eds.), *Primary Productivity and Biogeochemical Cycles in the Sea*, Vol. 43 of *Environmental Science Research*, Plenum Press, New York, pp. 69–88.

Cullen, J. J. (1990) On models of growth and photosynthesis in phytoplankton. *Deep-Sea Res.*, **37**, 667–683.

Doney, S. C. (1999) Major chalenges confronting marine biogeochemical modeling. *Global Biogeochem. Cycles*, **13**(3), 705–714.

Doney, S. C., Glover, D. M. and Najjar, R. G. (1996) A new coupled, one-dimensional biological-physical model for the upper ocean: applications to the JGOFS Bermuda Atlantic Time-series Study (BATS) site. *Deep-Sea Res.*, **43**(2-3), 591–629.

Doveri, F., Scheffer, M., Rinaldi, S., Muratori, S. and Kuznetsov, Y. (1993) Seasonality and chaos in a plankton-fish model. *Theor. Pop. Biol.*, **43**(2), 159–183.

Edwards, A. M. and Brindley, J. (1996) Oscillatory behaviour in a three-component plankton population model. *Dynamics and Stability of Systems*, **11**(4), 347–370.

Edwards, C. A., Powell, T. A. and Batchelder, H. P. (2000) The stability of an NPZ model subject to realistic levels of vertical mixing. *J. Mar. Res.*, **58**, 37–60.

Eppley, R. W. (1972) Temperature and phytoplankton growth in the sea. *Fish. Bull.*, **17**, 15–24.

Eppley, R. W. (1980) Estimating phytoplankton growth rates in the central oligotrophic oceans. In Falkowski, P. G. (ed.), *Primary Productivity in the Sea*, Vol. 19 of *Environmental Science Research*, Plenum Press, New York, pp. 231–240.

Eppley, R. W. and Peterson, B. J. (1979) Particulate organic matter flux and planktonic new production in the deep ocean. *Nature*, **282**, 677–679.

Eppley, R. W., Rogers, J. N. and McCarthy, J. J. (1969) Half-saturation constants for uptake of nitrate and ammonium by marine phytoplankton. *Limnol. Oceanogr.*, **14**, 912–920.

Eslinger, D. L. (1990) The effects of convective and wind-driven mixing on springtime phytoplankton dynamics as simulated by a mixed-layer model. Ph.D. thesis, Florida State University.

Evans, G. T. and Parslow, J. S. (1985) A model of annual plankton cycles. *Biol. Oceanogr.*, **3**(3), 327–347.

Fasham, M. J. R. (1995) Variations in the seasonal cycle of biological production in subarctic oceans: a model sensitivity analysis. *Deep-Sea Res.*, **42**(7), 1111–1149.

Fasham, M. J. R., Ducklow, H. W. and McKelvie, S. M. (1990) A nitrogen-based model of plankton dynamics in the oceanic mixed layer. *J. Mar. Res.*, **48**(3), 591–639.

Fasham, M. J. R., Sarmiento, J. L., Slater, R. D., Ducklow, H. W. and Williams, R. (1993) Ecosystem behavior at Bermuda Station S and Ocean Weather Station “India”: a general circulation model and observational analysis. *Global Biogeochem. Cycles*, **7**(2), 379–415.

Franks, P. J. S., Wroblewski, J. S. and Flierl, G. R. (1986) Behavior of a simple plankton model with food-level acclimation by herbivores. *Mar. Biol.*, **91**(1), 121–129.

Geider, R. J., MacIntyre, H. L. and Kana, T. M. (1997) Dynamic model of phytoplankton growth and

acclimation: responses of the balanced growth rate and the chlorophyll *a*:carbon ratio to light, nutrient limitation and temperature. *Mar. Ecol. Prog. Ser.*, **148**, 187–200.

Goulden, C. E. and Hornig, L. L. (1980) Population oscillations and energy reserves in planktonic cladocera and their consequences to competition. *Proceedings of the National Academy of Sciences, USA*, **77**, 1716–1720.

Hale, J. and Koçak, H. (1991) *Dynamics and Bifurcations*. Springer-Verlag, New York.

Hansen, P. J., Bjornsen, P. K. and Hansen, B. W. (1997) Zooplankton grazing and growth: scaling within the 2–2000 μm body size range. *Limnol. Oceanogr.*, **42**(4), 687–704.

Harrison, W. G. (1980) Nitrogen regeneration and primary production in the sea. In Falkowski, P. G. (ed.), *Primary Productivity in the Sea*, Vol. 19 of *Environmental Science Research*, Plenum Press, New York, pp. 433–460.

Harrison, W. G. (1992) Regeneration of nutrients. In Falkowski, P. G. and Woodhead, A. D. (eds.), *Primary Productivity and Biogeochemical Cycles in the Sea*, Vol. 43 of *Environmental Science Research*, Plenum Press, New York, pp. 385–407.

Hastings, A. and Powell, T. (1991) Chaos in a three-species food chain. *Ecology*, **72**(3), 896–903.

Hutchinson, G. E. (1961) The paradox of plankton. *Am. Nat.*, **95**, 137–144.

Kirk, J. T. O. (1992) The nature and measurement of the light environment in the ocean. In Falkowski, P. G. and Woodhead, A. D. (eds.), *Primary Productivity and Biogeochemical Cycles in the Sea*, Vol. 43 of *Environmental Science Research*, Plenum Press, New York, pp. 9–30.

Levin, S. A. (1978) Pattern formation in ecological communities. In Steele, J. H. (ed.), *Spatial Pattern in*

Plankton Communities, Vol. 3 of *NATO Conference Series IV: Marine Sciences*, Plenum Press, New York, pp. 467–465.

List, R. J. (1971) *Smithsonian Meteorological Tables*, Vol. 114 of *Smithsonian Miscellaneous Collections*. Smithsonian Institution Press, Washington.

Marra, J., Bidigare, R. R. and Dickey, T. D. (1990) Nutrients and mixing, chlorophyll and phytoplankton growth. *Deep-Sea Res.*, **37**, 127–143.

May, R. (1973) *Stability and complexity in model ecosystems*, Vol. 6 of *Monographs in Population Biology*. Princeton University Press, Princeton, N.J.

McCann, K. and Yodzis, P. (1994) Biological conditions for chaos in a three-species food chain. *Ecology*, **75**(2), 561–564.

McCarthy, J. J. and Carpenter, E. J. (1983) Nitrogen cycling in near-surface waters of the open ocean. In Carpenter, E. J. and Capone, D. G. (eds.), *Nitrogen in The Marine Environment*, Academic Press, New York, pp. 487–512.

McCauley, E. and Murdoch, W. W. (1987) Cyclic and stable populations: plankton as a paradigm. *Am. Nat.*, **129**, 97–121.

McCreary, J. P., Kohler, K. E., Hood, R. R. and Olson, D. B. (1996) A four-component ecosystem models of biological activity in the Arabian Sea. *Prog. Oceanogr.*, **37**, 193–240.

McGillicuddy, D. J., Robinson, A. R., Siegel, D. A., Jannasch, H. W., Johnson, R., Dickey, T. D., McNeil, J., Michaels, A. F. and Knap, A. H. (1998) Influence of mesoscale eddies on new production in the Sargasso Sea. *Nature*, **394**, 263–266.

Moloney, C. L. and Field, J. G. (1991) The size-based dynamics of plankton food webs. i. a simulation model of carbon and nitrogen flows. *J. Plankton Res.*, **13**, 1003–1038.

Moore, J. K., Doney, S., Kleypas, J. A., Glover, D. M. and Fung, I. Y. (2000) An intermediate complexity marine ecosystem model for the global domain. *DSR II*. Submitted.

Okubo, A. (1978) Horizontal dispersion and critical scales for phytoplankton. In Steele, J. H. (ed.), *Spatial Pattern in Plankton Communities*, Vol. 3 of *NATO Conference Series IV: Marine Sciences*, Plenum Press, New York, pp. 21–42.

Olson, D. B. and Hood, R. R. (1994) Modellling pelagic biogeography. *Prog. Oceanogr.*, **34**, 161–205.

Olson, D. B., Lima, I. D., Peng, G. and Davis, C. (2001) Instability of planktonic food chains and the deep chlorophyll maximum. *In preparation*.

Orr, J. C. and Sarmiento, J. L. (1992) Potential of marine macroalgae as a sink for CO_2: Constraints from a 3-D general circulation model of the global ocean. *Water Air and Soil Pollution*, **64**(1-2), 405–421.

Oschlies, A. and Garçon, V. (1998) Eddy-induced enhancement of primary production in a model of the North Atlantic Ocean. *Nature*, **394**, 266–269.

Oschlies, A. and Garçon, V. (1999) An eddy-permiting coupled physical-biological models of the North Atlantic. 1. sensitivity to advection numerics and mixed layer. *Global Biogeochem. Cycles*, **13**(1), 135–160.

Parsons, T. R., Takahashi, M. and Hargrave, B. (1984) *Biological Oceanographic Processes*. Pergamon Press, Oxford.

Pascual, M. (1993) Diffusion-induced chaos in a spatial predator-prey system. *Proc. R. Soc. London Ser. B*, **251**, 1–7.

Peterson, D. H., Perry, M. J., Bencala, K. E. and Talbot, M. C. (1987) Phytoplankton productivity in relation to light intensity: a simple equation. *Est. Coast. Shelf Sci.*, **24**, 813–832.

Platt, T., Sathyendranath, S., Ulloa, O., Harrison, W. G., Hoepffner, N. and Goes, J. (1992) Nutrient control of phytoplankton photosynthesis in the Western North Atlantic. *Nature*, **352**, 220–231.

Platt, T., Subba Rao, D. V. and Irwin, B. (1983) Photosynthesis of picoplankton in the oligotrophic ocean. *Nature*, **301**, 702–704.

Pomeroy, L. (1974) The ocean's food web, a changing paradigm. *BioScience*, **24**, 499–504.

Prezelin, B. B., Tilzer, M. M., Schofield, O. and Haese, C. (1991) The control of the production processes of phytoplankton by the physical structure of the aquatic environment with special reference to its optical propoerties. *Aquat. Sci.*, **53**, 136–186.

Rand, D. and Wilson, H. (1991) Chaotic stochasticity: A ubiquitous source of unpredictability in epidemics. *Proc. R. Soc. London Ser. B*, **246**, 179–184.

Rosenzeig, M. L. (1971) Paradox of enrichment: destabilization of exploitation ecosystems in ecological time. *Science*, **171**, 385–387.

Roughgarden, J. and Feldman, M. (1975) Species packing and predation pressure. *Ecology*.

Ryabchenko, V. A., Fasham, M. J. R., Kagan, B. A. and Popova, E. E. (1997) What causes short-term oscillations in ecosystem models of the ocean mixed layer? *J. Mar. Syst.*, **13**, 33–50.

Sarmiento, J. L., Slater, R. D., Fasham, M. J. R., Ducklow, H. W., Toggweiler, J. R. and Evans, G. T. (1993) A seasonal three-dimensional ecosystem model of nitrogen cycling in the North Atlantic euphotic zone. *Global Biogeochem. Cycles*, **7**(2), 417–450.

Schaffer, W. M. (1985) Order and chaos in ecological systems. *Ecology*, **66**, 93–106.

Sieburth, J. M. (1982) Grazing of bacteria by protozooplankton in pelagic marine waters. In Hobbie, J. E. and Williams, A. J. L. B. (eds.), *Heterotrophic Activity in the Sea*, Vol. 15 of *NATO Conference Series IV: Marine Sciences*, Plenum Press, New York, pp. 405–444.

Sorokin, Y. I. (1981) Microheterotrophic organisms in marine ecosystems. In Longhurst, A. R. (ed.), *Analysis of Marine Ecosystems*, Academic Press, New York, pp. 293–342.

Steele, J. H. and Henderson, E. W. (1992) The role of predation in plankton models. *J. Plankton Res.*, **14**(1), 157–172.

Venrick, E. L. (1986) Patchiness and the paradox of the plankton. In Pierrot-Bults, A. C., van der Spoel, S., Zahuranec, B. J. and Johnson, R. K. (eds.), *Pelagic Biogeography*, Vol. 49 of *UNESCO Technical Papers in Marine Science*, UNESCO, Paris, pp. 261–165.

Venrick, E. L. (1988) The vertical distribution of chlorophyll and phytoplankton species in the North Pacific central environment. *J. Plankton Res.*, **10**, 987–998.

Venrick, E. L. (1990) Phytoplankton in an oligotrophic ocean: species structure and interannual variability. *Ecology*, **71**(4), 1547–1563.

Williams, R. (1988) Spatial heterogeneity and niche differentiation in oceanic zooplankton. In Boxshall, G. A. and Schimke, H. K. (eds.), *Biology of Copepods: Proceedings of the Third International Conference*

on Copepoda, Vol. 47 of *Developments in Hydrobiology*, Kluwer Academic Publishers, Boston, pp. 151–159.

Wroblewski, J. S. (1989) A model of the spring bloom in the North Atlantic and its impact on ocean optics. *Limnol. Oceanogr.*, **34**, 1563–1571.

Figure Captions

Fig. 1: Structure of biological models.

Fig. 2: Equilibrium values of the different compartments in the NPZD (single-species) model with fixed preferences as function of total nitrogen in the system (N_0) and light (photosynthetically available radiation, I_{par}). (a) phytoplankton, (b) zooplankton, (c) dissolved nutrients, (d) detritus. Units are W m^{-2} (I_{par}) and mMol N m^{-3} (N_0). Light variation (horizontal axis) is presented in logarithmic scale and shaded gray area indicates where system becomes unstable.

Fig. 3: Phase diagram of NPZD model showing the asymptotically stable equilibrium solution at $N_0 = 2$ mMol N m^{-3} and the limit cycle at $N_0 = 9$ mMol N m^{-3}, for $I_{par} = 14$ W m^{-2}.

Fig. 4: Position of equilibrium points of NPZD (single-species) model with fixed preferences in the predation functional response as function of light availability (photosynthetically available radiation, I_{par}) (a) $N_0 = 2$ mMol N m^{-3}, (b) $N_0 = 9$ mMol N m^{-3}. I_{par} units are W m^{-2}.

Fig. 5: The time evolution of the NPZD model with fixed preferences in the predation functional response at light intensities equivalent to that at the depths of 25, 50, 75 and 100 meters ($N_0 = 2$ mMol N m^{-3}).

Fig. 6: Equilibrium values of the different compartments in the NPZD (single-species) model with variable preferences as function of total nitrogen in the system (N_0) and light (photosynthetically available radiation, I_{par}). (a) phytoplankton, (b) zooplankton, (c) dissolved nutrients, (d) detritus. Units are W m^{-2} (I_{par}) and mMol N m^{-3} (N_0). Light variation (horizontal axis) is presented in logarithmic scale.

Fig. 7: Position of equilibrium points of NPZD (single-species) model with fixed preferences in the predation functional response as function of light availability (photosynthetically available radiation, I_{par}) (a) $N_0 = 2$ mMol N m^{-3}, (b) $N_0 = 9$ mMol N m^{-3}. Units are W m^{-2} (I_{par}).

Fig. 8: The time evolution of the NPZD model with variable preferences in the predation functional response at light intensities equivalent to that at the depths of 25, 50, 75 and 100 meters ($N_0 = 2$ mMol N m^{-3}).

Fig. 9: Equilibrium values of the different compartments in the NPPZD model with fixed preferences as function of total nitrogen in the system (N_0) and light (photosynthetically available radiation, I_{par}). (a) small phytoplankton, (b) large phytoplankton, (c) dissolved nutrients, (d) zooplankton. Units are W m^{-2} (I_{par}) and mMol N m^{-3} (N_0). Light variation (horizontal axis) is presented in logarithmic scale and shaded gray area indicates where system becomes unstable.

Fig. 10: Position of equilibrium points of NPPZD model with fixed preferences as function of light availability (photosynthetically available radiation, I_{par}) (a) $N_0 = 2.5$ mMol N m^{-3}), (b) $N_0 = 9$ mMol N m^{-3}. I_{par} units are W m^{-2}.

Fig. 11: Equilibrium values of the different compartments in the NPPZD model with variable preferences as function of total nitrogen in the system (N_0) and light (photosynthetically available radiation, I_{par}). (a) small phytoplankton, (b) large phytoplankton, (c) dissolved nutrients, (d) zooplankton. Units are W m^{-2} (I_{par}) and mMol N m^{-3} (N_0). Light variation (horizontal axis) is presented in logarithmic scale and shaded gray area indicates where system becomes unstable.

Fig. 12: Position of equilibrium points of NPPZD model with variable preferences as function of light availability (photosynthetically available radiation, I_{par}) (a) $N_0 = 2.5$ mMol N m^{-3}), (b) $N_0 = 9$ mMol N m^{-3}. I_{par} units are W m^{-2}.

Fig. 13: Equilibrium values of the different compartments in the NPPZZD model with variable preferences as function of total nitrogen in the system (N_0) and light (photosynthetically available radiation, I_{par}). (a) small phytoplankton, (b) large phytoplankton, (c) small zooplankton, (d) large zooplankton, (e) dissolved

nutrients, (f) detritus. Units are W m^{-2} (I_{par}) and mMol N m^{-3} (N_0). Light variation (horizontal axis) is presented in logarithmic scale and shaded gray area indicates where system becomes unstable.

Fig. 14: Position of equilibrium points of NPPZZD model with variable preferences as function of light availability (photosynthetically available radiation, I_{par}) (a) $N_0 = 2.5$ mMol N m^{-3}), (b) $N_0 = 9$ mMol N m^{-3}. I_{par} units are W m^{-2}.

Fig. 15: The time evolution of the NPPZZD model with variable preferences from initially low concentrations of P_1, P_2, Z_1 and Z_2 (0.1 mMol N m^{-3}) and high concentration of N (2 mMol N m^{-3}), at light intensities equivalent to that at the depths of 25, 50, 75 and 100 meters ($N_0 = 2.5$ mMol N m^{-3}).

Fig. 16: The time evolution of total phytoplankton ($P_1 + P_2$), total zooplankton ($Z_1 + Z_2$), detritus (D) and dissolved nutrients (N) from NPPZZD mode with variable preferences, form initially low concentrations of P_1, P_2, Z_1 and Z_2 (0.1 mMol N m^{-3}) and high concentration of N (2 mMol N m^{-3}), at light intensities equivalent to that at the depths of 25, 50, 75 and 100 meters ($N_0 = 2.5$ mMol N m^{-3}).

Fig. 17: Ratio between the growth rates of predator (zooplankton, μ_{Z_i}) and prey (phytoplankton, μ_{P_i} and small zooplankton, $\mu_{Z_{i-1}}$) in the different model formulations with variable preferences in the functional response, at varying light intensities (I_{par}). Total nitrogen concentration (N_0) is 9 mMol N m^{-3}. The range of light intensities where the systems oscillate in a limit cycle is denoted by a sharp drop in the ratio between predator (Z_i) and prey (P_i or Z_{i-1}) growth rates. In the unstable region, the growth rates for the different compartments were computed at the same point in the limit cycle.

Fig. 18: Position of equilibrium points of the different compartments in the NPPZZD and NPZD models, with variable preferences, as function of light availability (photosynthetically available radiation, I_{par}) for $N_0 = 2.5$ mMol N m^{-3}. Single-species model: dissolved nitrogen (N_s), phytoplankton (P), zooplankton (Z),

and detritus (D_s). NPPZZD model: small phytoplankton (P_1), large phytoplankton (P_2), total phytoplankton ($P_1 + P_2$), small zooplankton (Z_1), large zooplankton (Z_2), total zooplankton ($Z_1 + Z_2$), detritus (D_m), and dissolved nutrients (N_m). Units are W m^{-2} (I_{par}) and mMol N m^{-3}.

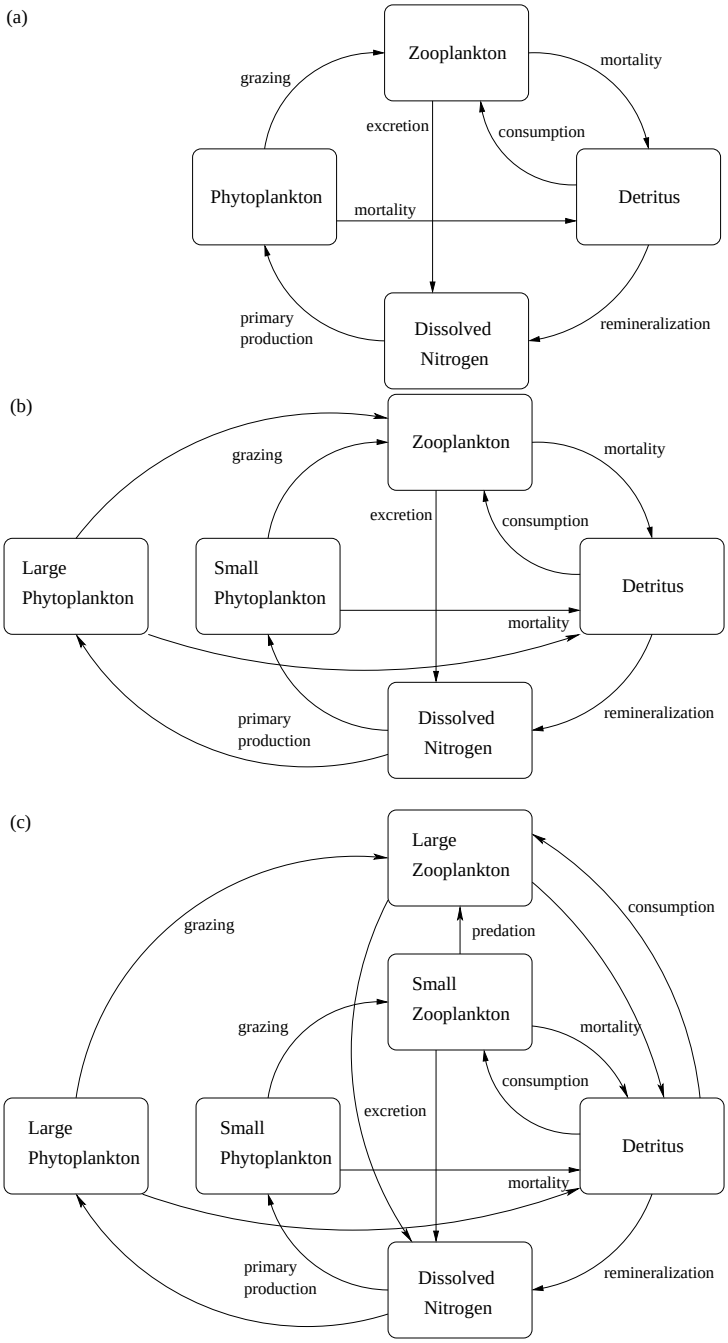

Figure 1: Structure of biological models.

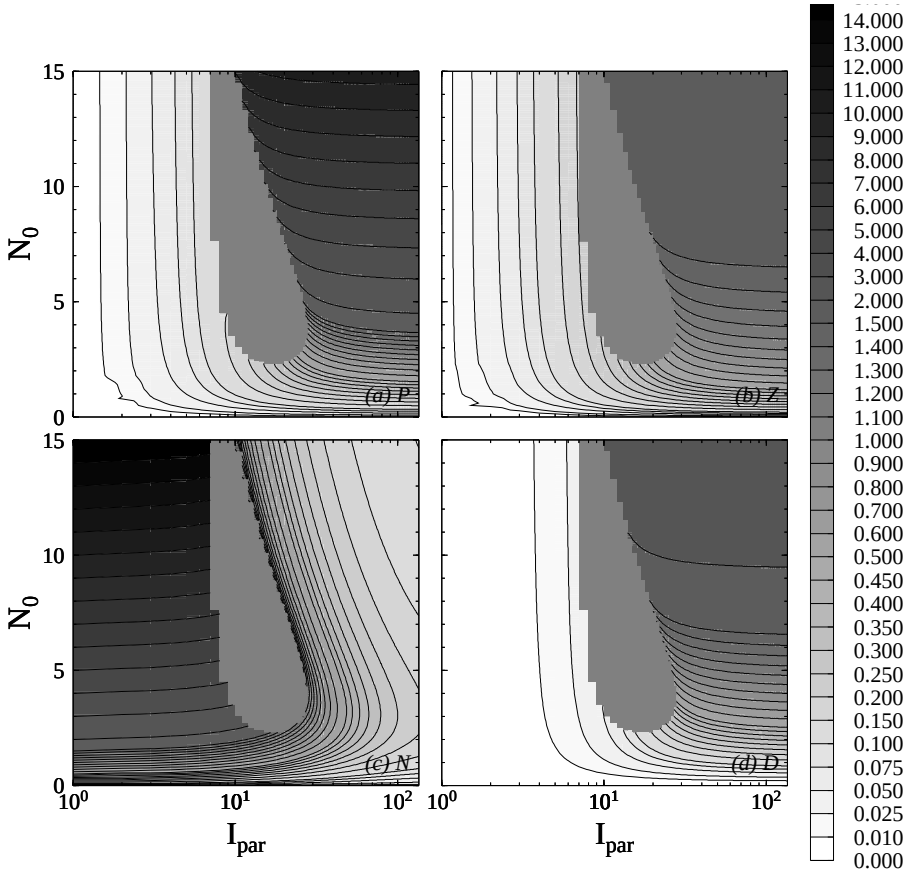

Figure 2: Equilibrium values of the different compartments in the NPZD (single-species) model with fixed preferences as function of total nitrogen in the system (N_0) and light (photosynthetically available radiation, I_{par}). (a) phytoplankton, (b) zooplankton, (c) dissolved nutrients, (d) detritus. Units are W m^{-2} (I_{par}) and mMol N m^{-3} (N_0). Light variation (horizontal axis) is presented in logarithmic scale and shaded gray area indicates where system becomes unstable.

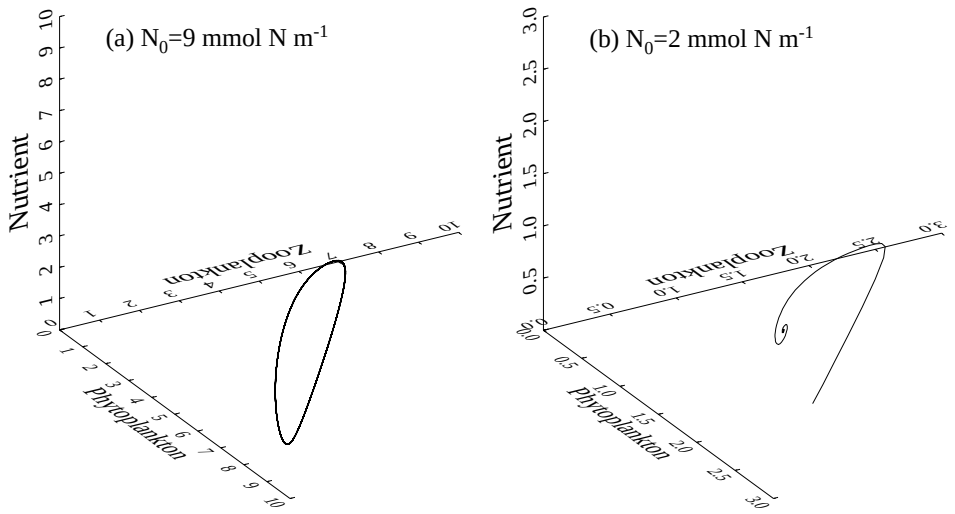

Figure 3: Phase diagram of NPZD model showing the asymptotically stable equilibrium solution at $N_0 = 2$ mMol N m^{-3} and the limit cycle at $N_0 = 9$ mMol N m^{-3}, for $I_{par} = 14$ W m^{-2}.

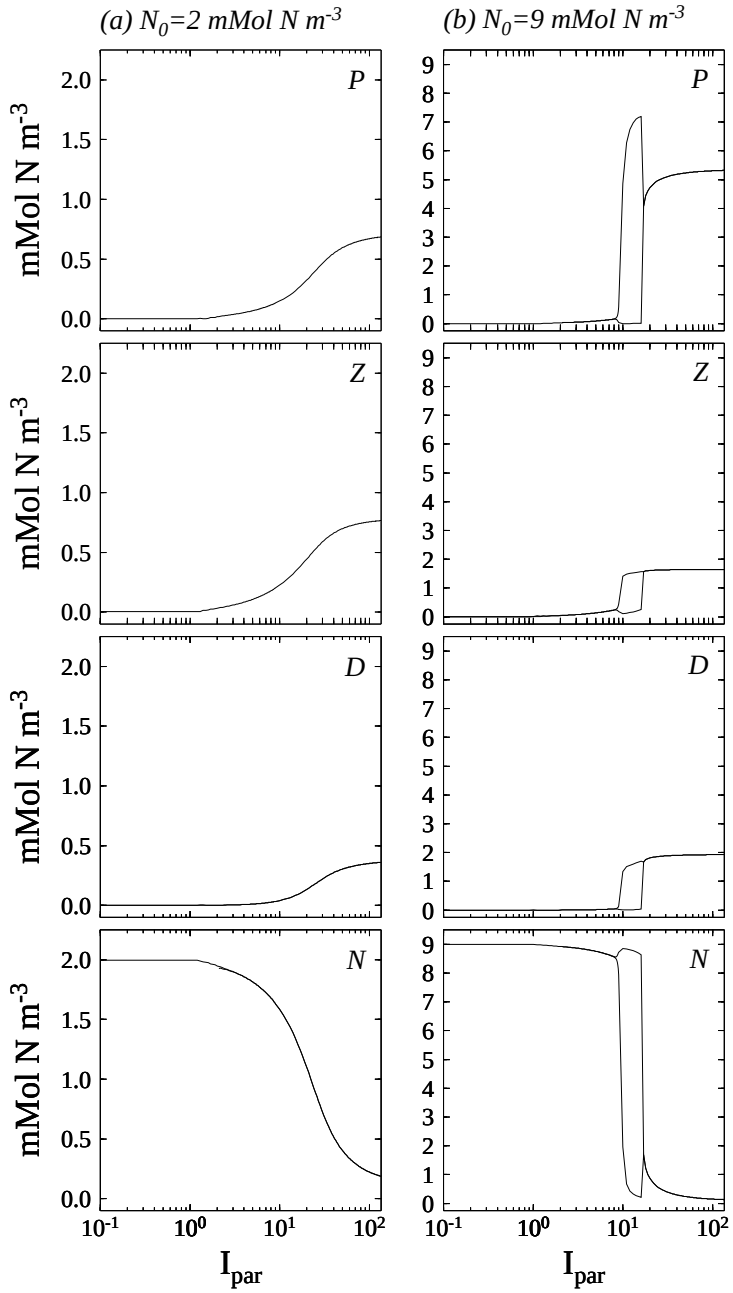

Figure 4: Position of equilibrium points of NPZD (single-species) model with fixed preferences in the predation functional response as function of light availability (photosynthetically available radiation, I_{par}) (a) $N_0 = 2$ mMol N m^{-3}, (b) $N_0 = 9$ mMol N m^{-3}. I_{par} units are W m^{-2}.

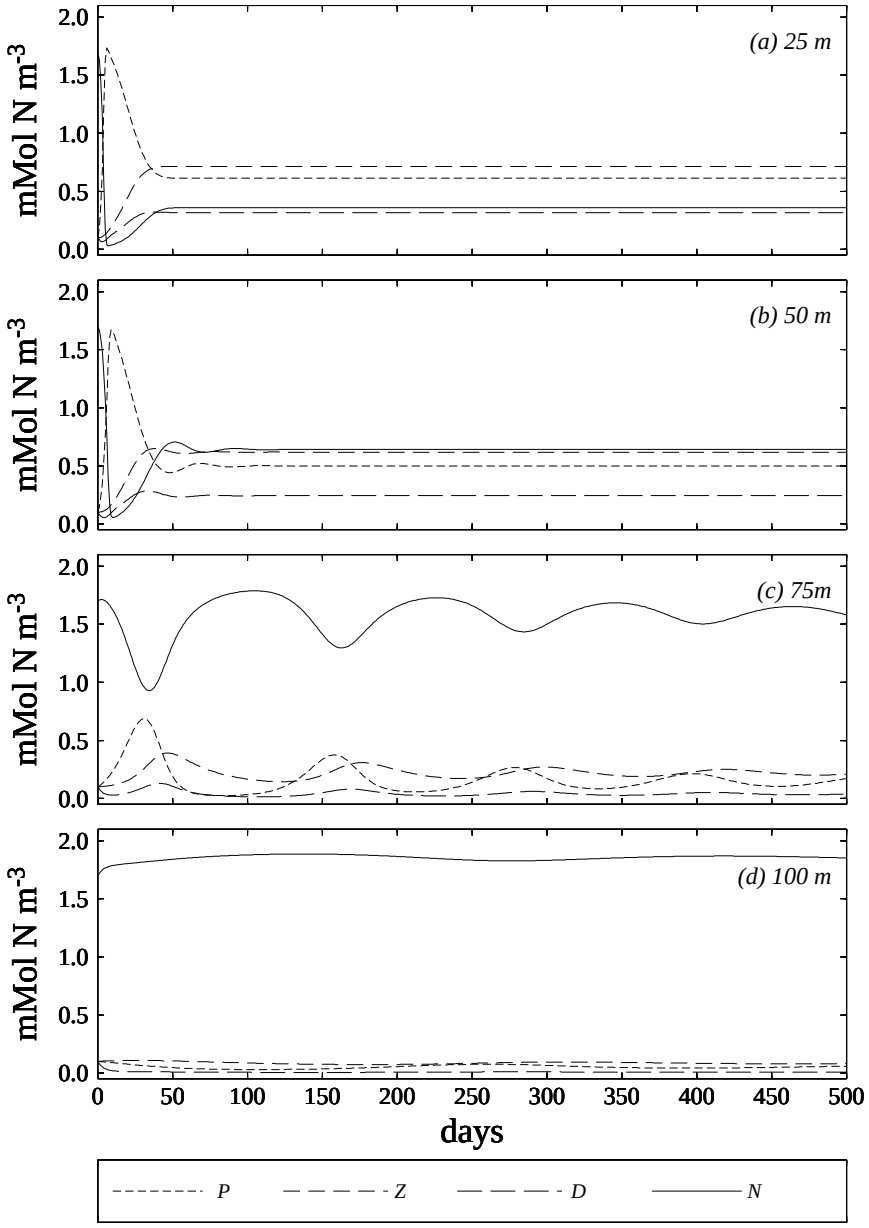

Figure 5: The time evolution of the NPZD model with fixed preferences in the predation functional response at light intensities equivalent to that at the depths of 25, 50, 75 and 100 meters ($N_0 = 2$ mMol N m^{-3}).

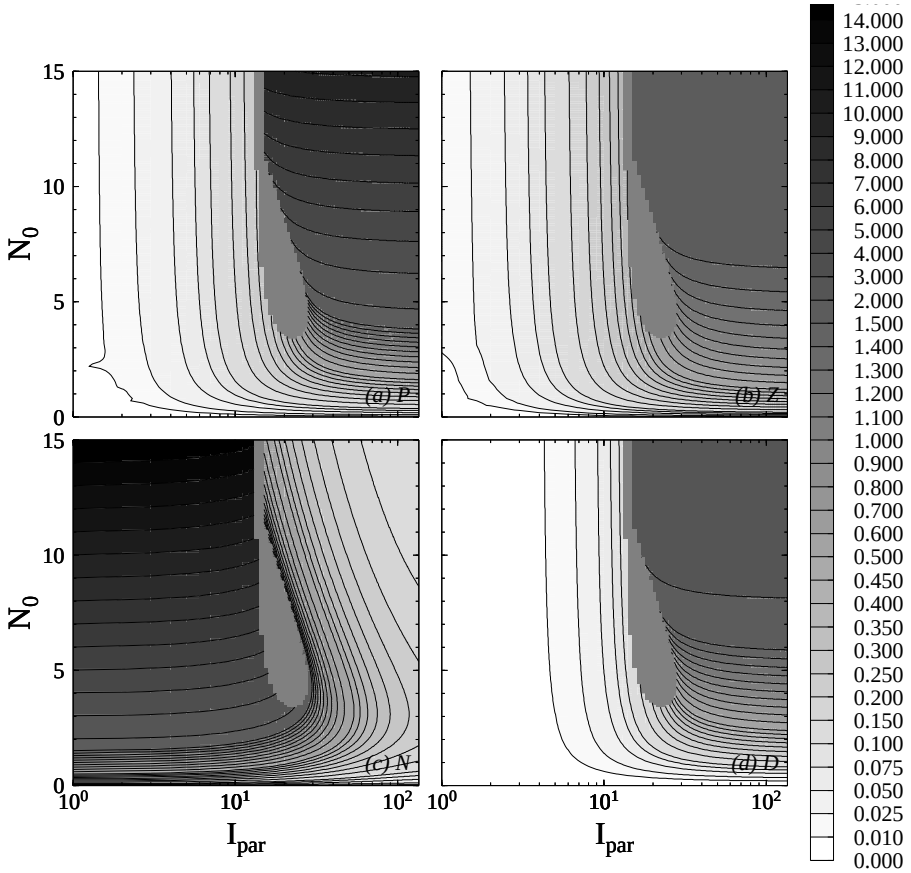

Figure 6: Equilibrium values of the different compartments in the NPZD (single-species) model with variable preferences as function of total nitrogen in the system (N_0) and light (photosynthetically available radiation, I_{par}). (a) phytoplankton, (b) zooplankton, (c) dissolved nutrients, (d) detritus. Units are W m^{-2} (I_{par}) and mMol N m^{-3} (N_0). Light variation (horizontal axis) is presented in logarithmic scale.

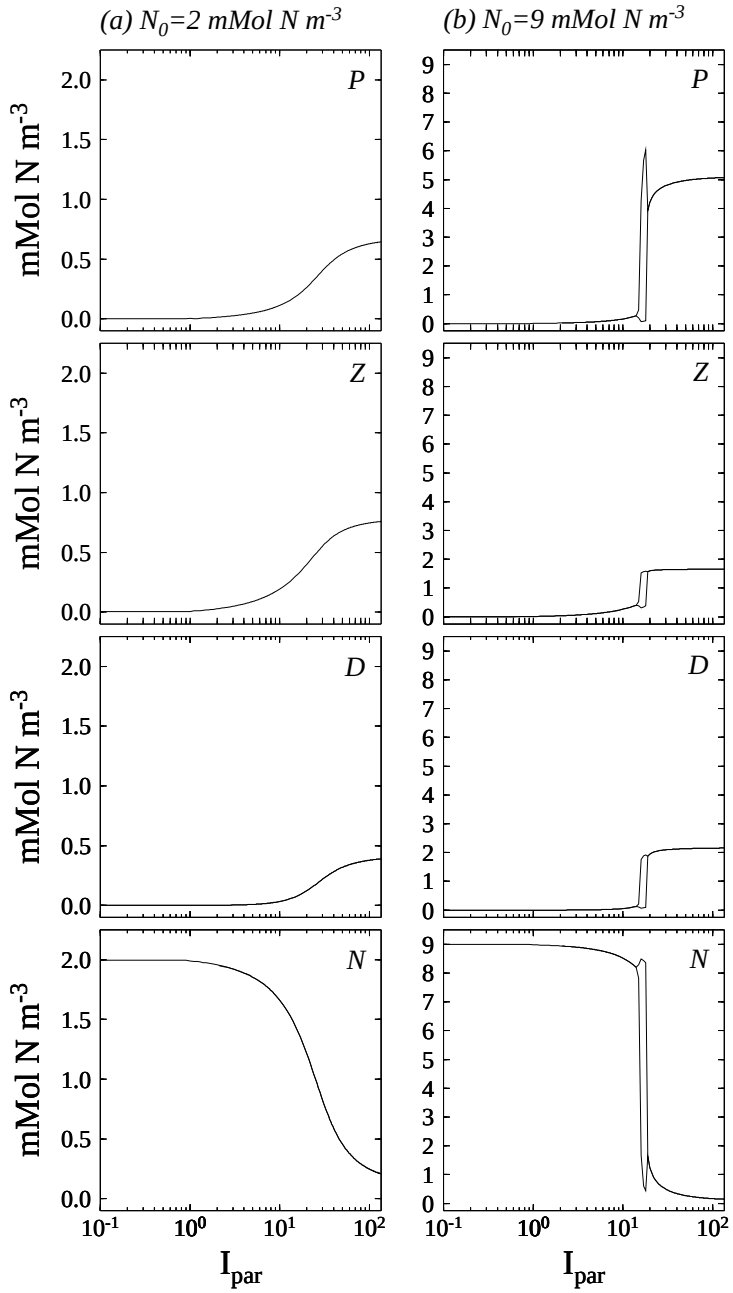

Figure 7: Position of equilibrium points of NPZD (single-species) model with fixed preferences in the predation functional response as function of light availability (photosynthetically available radiation, I_{par}) (a) $N_0 = 2$ mMol N m^{-3}, (b) $N_0 = 9$ mMol N m^{-3}. Units are W m^{-2} (I_{par}).

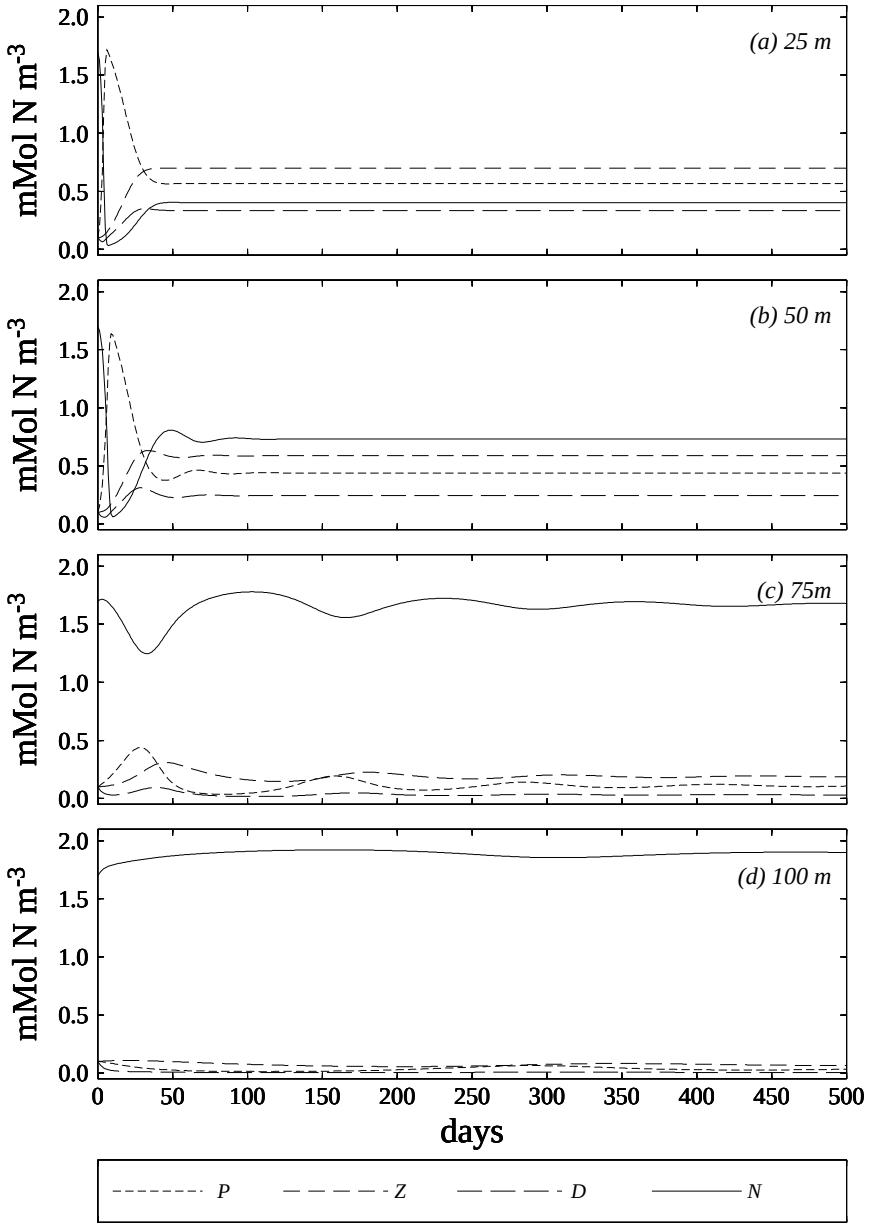

Figure 8: The time evolution of the NPZD model with variable preferences in the predation functional response at light intensities equivalent to that at the depths of 25, 50, 75 and 100 meters ($N_0 = 2$ mMol N m^{-3}).

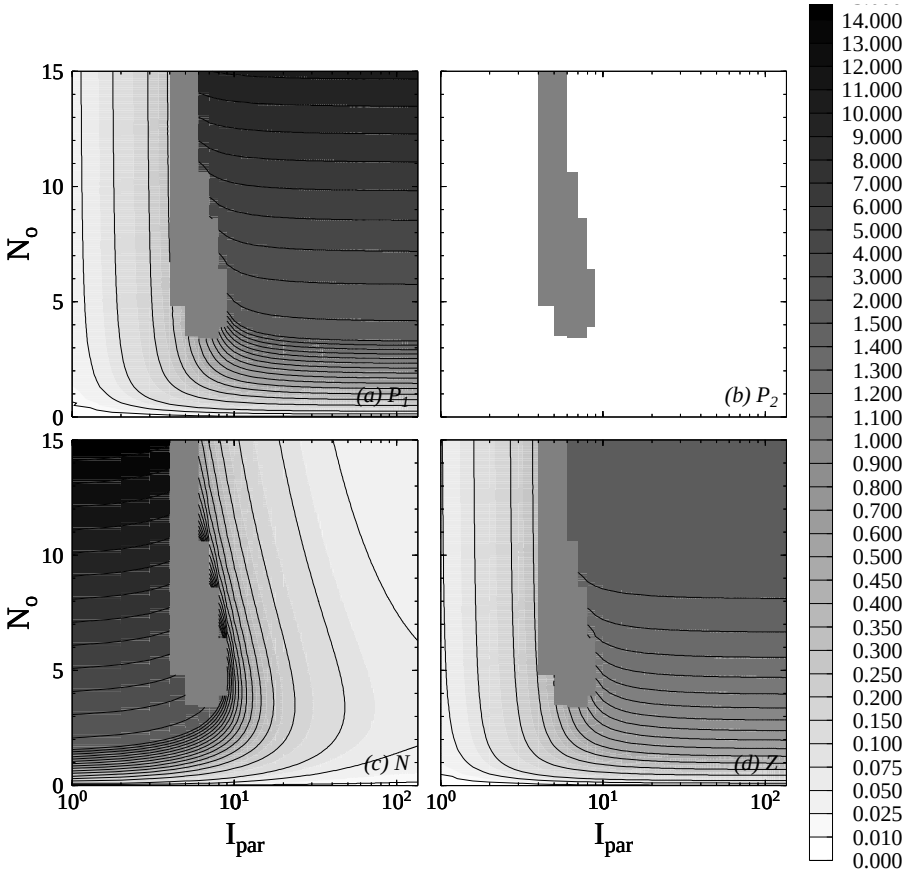

Figure 9: Equilibrium values of the different compartments in the NPPZD model with fixed preferences as function of total nitrogen in the system (N_0) and light (photosynthetically available radiation, I_{par}). (a) small phytoplankton, (b) large phytoplankton, (c) dissolved nutrients, (d) zooplankton. Units are W m^{-2} (I_{par}) and mMol N m^{-3} (N_0). Light variation (horizontal axis) is presented in logarithmic scale and shaded gray area indicates where system becomes unstable.

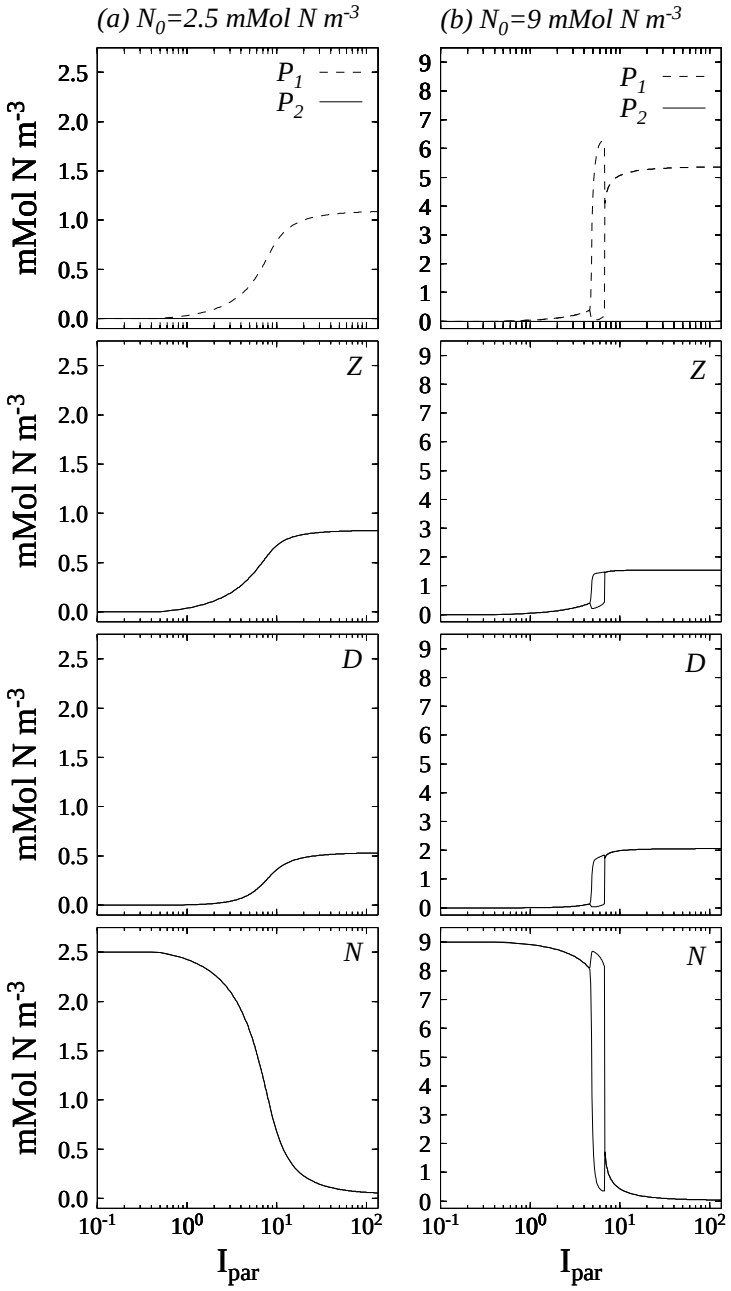

Figure 10: Position of equilibrium points of NPPZD model with fixed preferences as function of light availability (photosynthetically available radiation, I_{par}) (a) $N_0 = 2.5$ mMol N m^{-3}), (b) $N_0 = 9$ mMol N m^{-3}. I_{par} units are W m^{-2}.

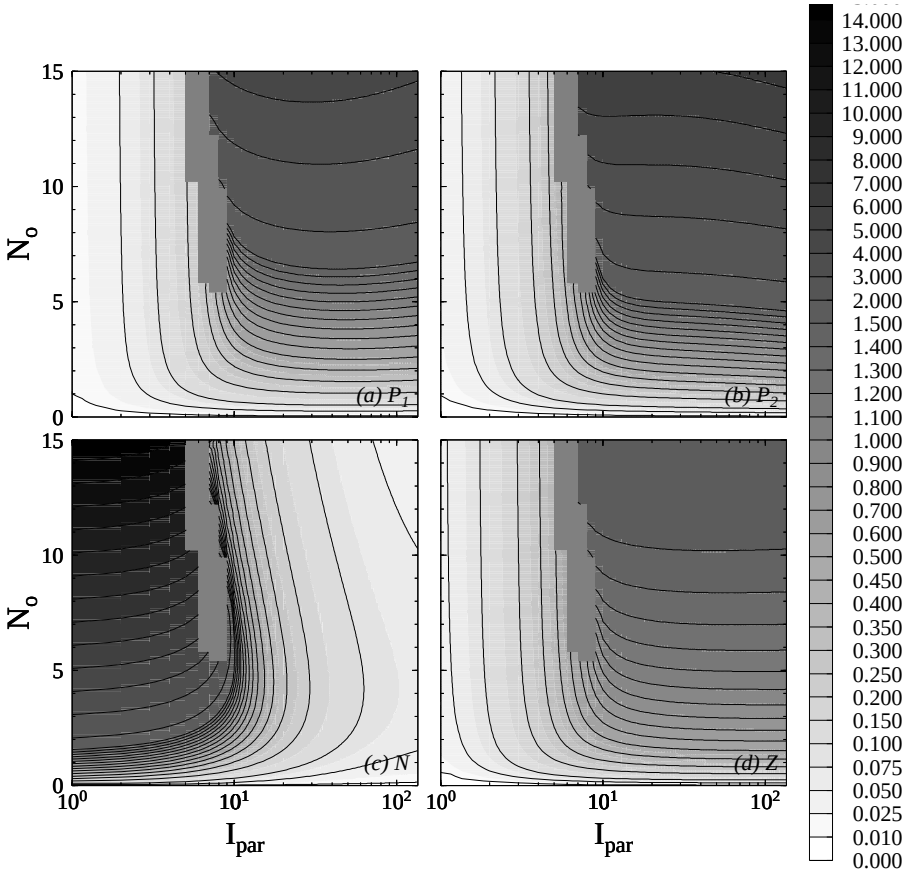

Figure 11: Equilibrium values of the different compartments in the NPPZD model with variable preferences as function of total nitrogen in the system (N_0) and light (photosynthetically available radiation, I_{par}). (a) small phytoplankton, (b) large phytoplankton, (c) dissolved nutrients, (d) zooplankton. Units are W m^{-2} (I_{par}) and mMol N m^{-3} (N_0). Light variation (horizontal axis) is presented in logarithmic scale and shaded gray area indicates where system becomes unstable.

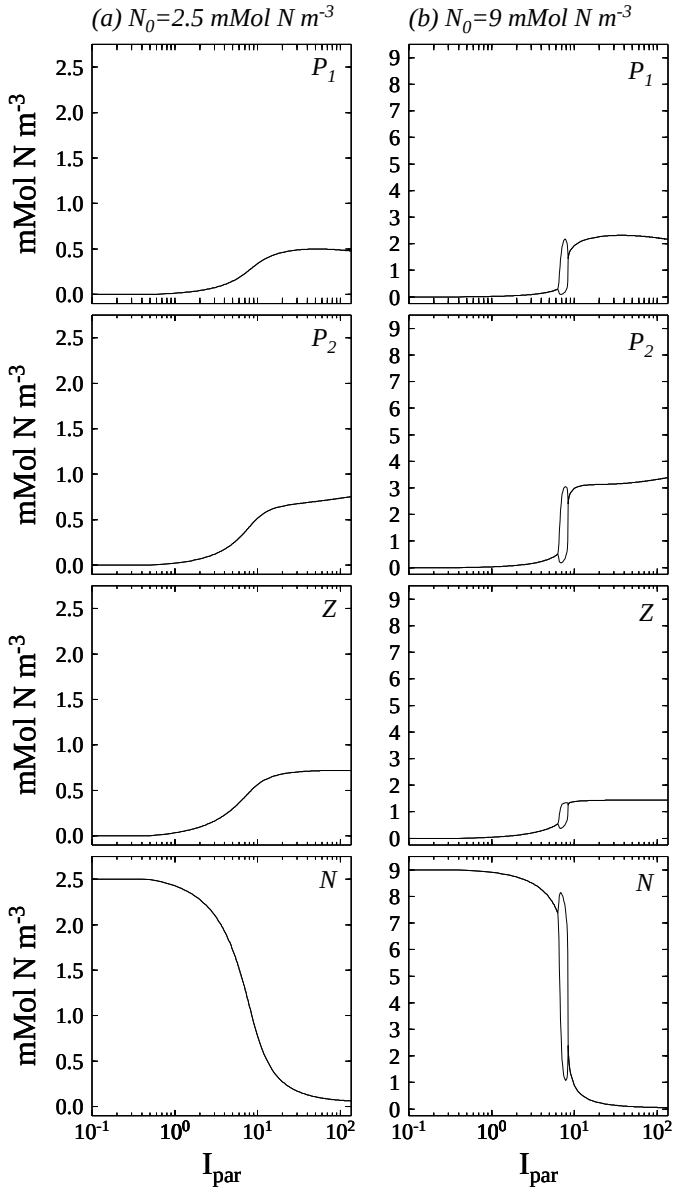

Figure 12: Position of equilibrium points of NPPZD model with variable preferences as function of light availability (photosynthetically available radiation, I_{par}) (a) $N_0 = 2.5$ mMol N m^{-3}), (b) $N_0 = 9$ mMol N m^{-3}. I_{par} units are W m^{-2}.

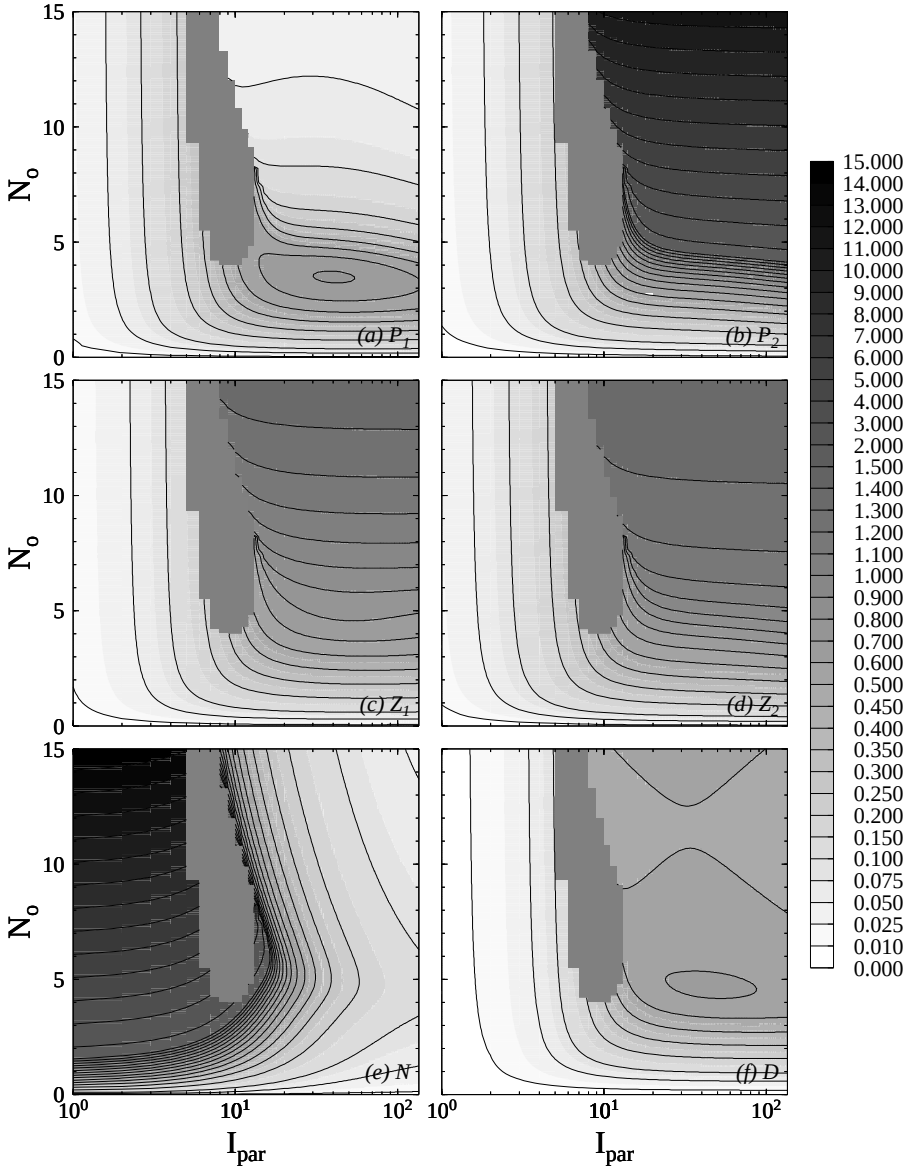

Figure 13: Equilibrium values of the different compartments in the NPPZZD model with variable preferences as function of total nitrogen in the system (N_0) and light (photosynthetically available radiation, I_{par}). (a) small phytoplankton, (b) large phytoplankton, (c) small zooplankton, (d) large zooplankton, (e) dissolved nutrients, (f) detritus. Units are W m^{-2} (I_{par}) and mMol N m^{-3} (N_0). Light variation (horizontal axis) is presented in logarithmic scale and shaded gray area indicates where system becomes unstable.

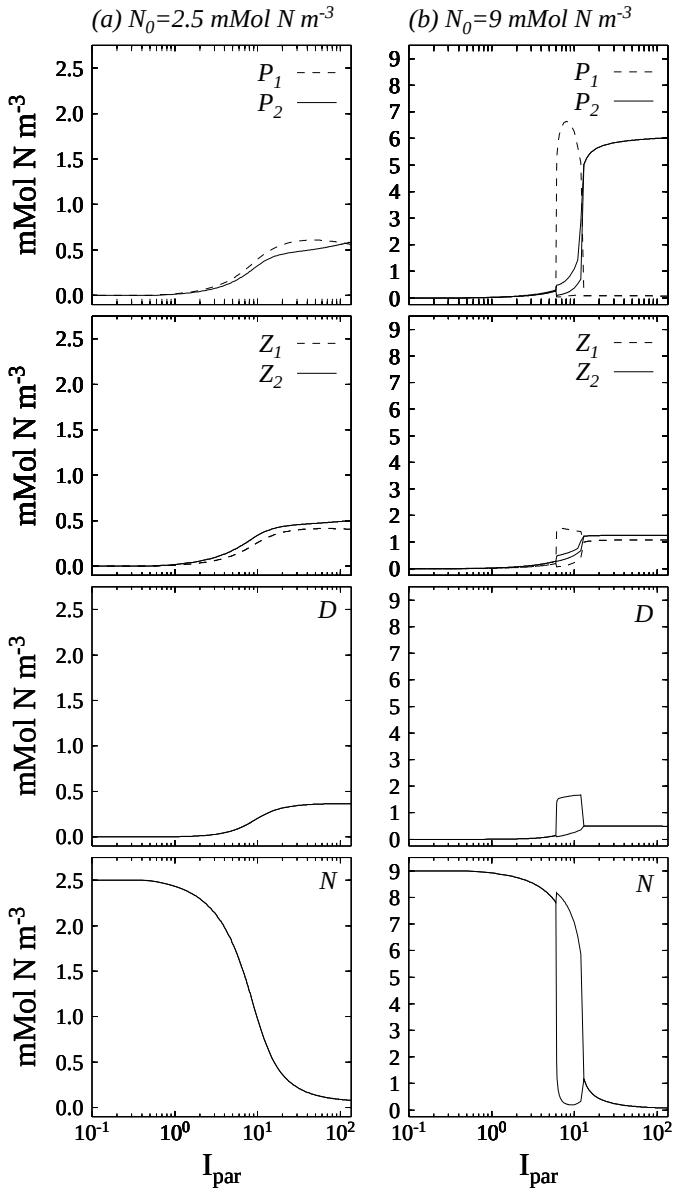

Figure 14: Position of equilibrium points of NPPZZD model with variable preferences as function of light availability (photosynthetically available radiation, I_{par}) (a) $N_0 = 2.5$ mMol N m^{-3}), (b) $N_0 = 9$ mMol N m^{-3}. I_{par} units are W m^{-2}.

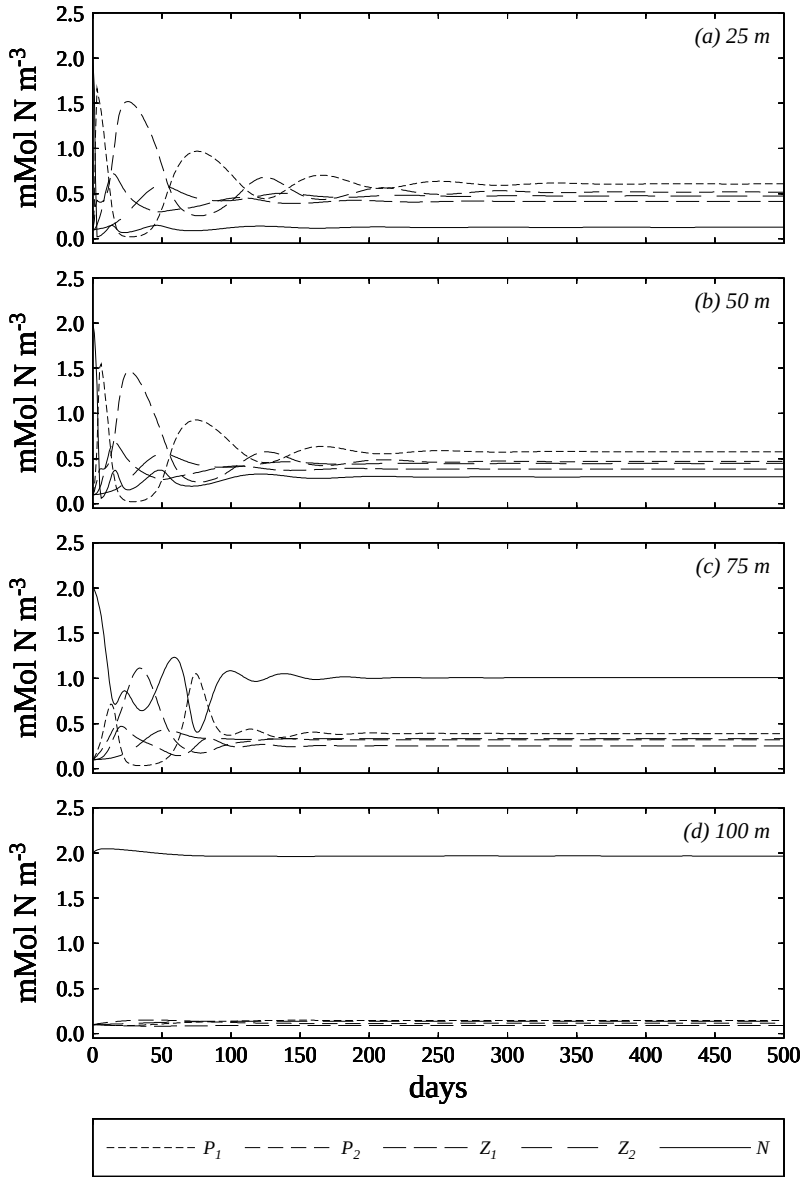

Figure 15: The time evolution of the NPPZZD model with variable preferences from initially low concentrations of P_1, P_2, Z_1 and Z_2 (0.1 mMol N m^{-3}) and high concentration of N (2 mMol N m^{-3}), at light intensities equivalent to that at the depths of 25, 50, 75 and 100 meters ($N_0 = 2.5$ mMol N m^{-3}).

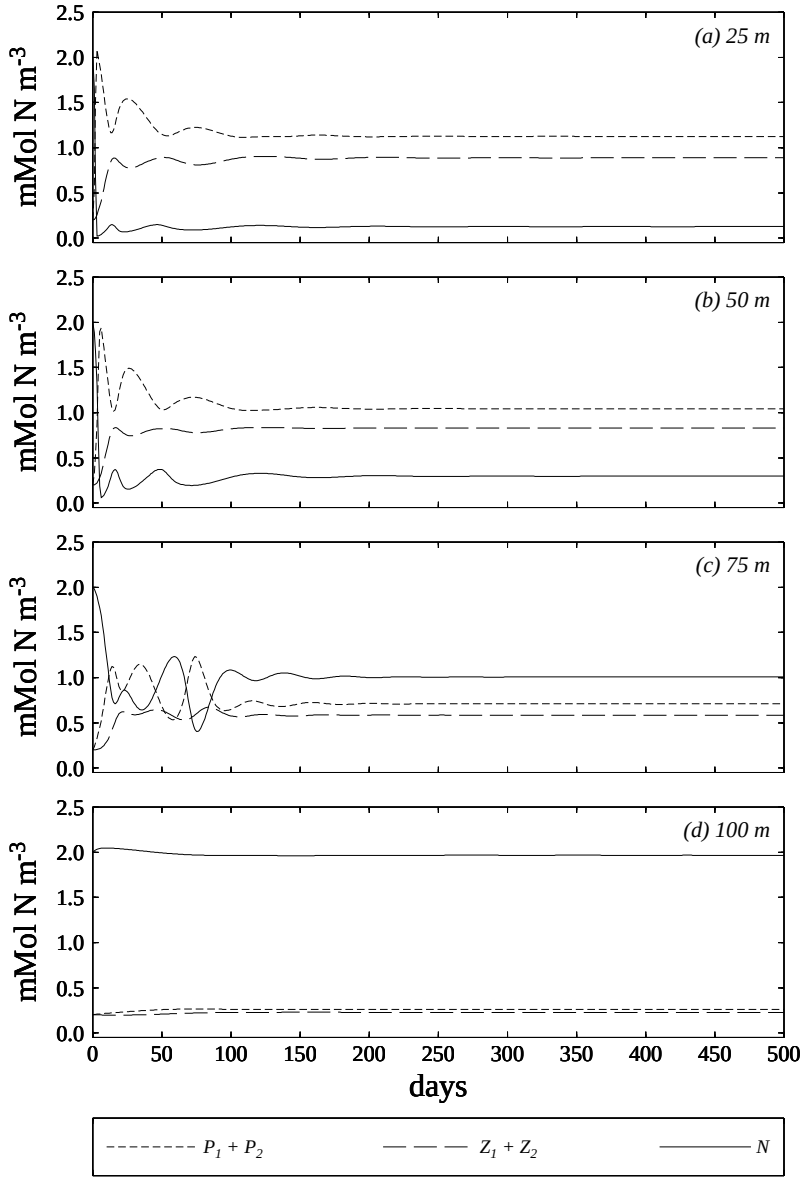

Figure 16: The time evolution of total phytoplankton ($P_1 + P_2$), total zooplankton ($Z_1 + Z_2$), detritus (D) and dissolved nutrients (N) from NPPZZD mode with variable preferences, form initially low concentrations of P_1, P_2, Z_1 and Z_2 (0.1 mMol N m^{-3}) and high concentration of N (2 mMol N m^{-3}), at light intensities equivalent to that at the depths of 25, 50, 75 and 100 meters ($N_0 = 2.5$ mMol N m^{-3}).

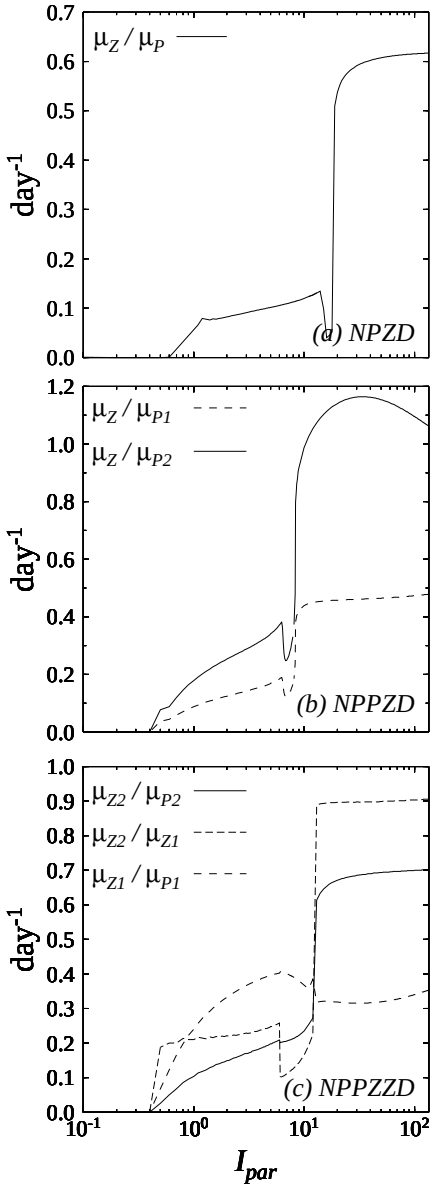

Figure 17: Ratio between the growth rates of predator (zooplankton, μ_{Z_i}) and prey (phytoplankton, μ_{P_i} and small zooplankton, $\mu_{Z_{i-1}}$) in the different model formulations with variable preferences in the functional response, at varying light intensities (I_{par}). Total nitrogen concentration (N_0) is 9 mMol N m^{-3}. The range of light intensities where the systems oscillate in a limit cycle is denoted by a sharp drop in the ratio between predator (Z_i) and prey (P_i or Z_{i-1}) growth rates. In the unstable region, the growth rates for the different compartments were computed at the same point in the limit cycle.

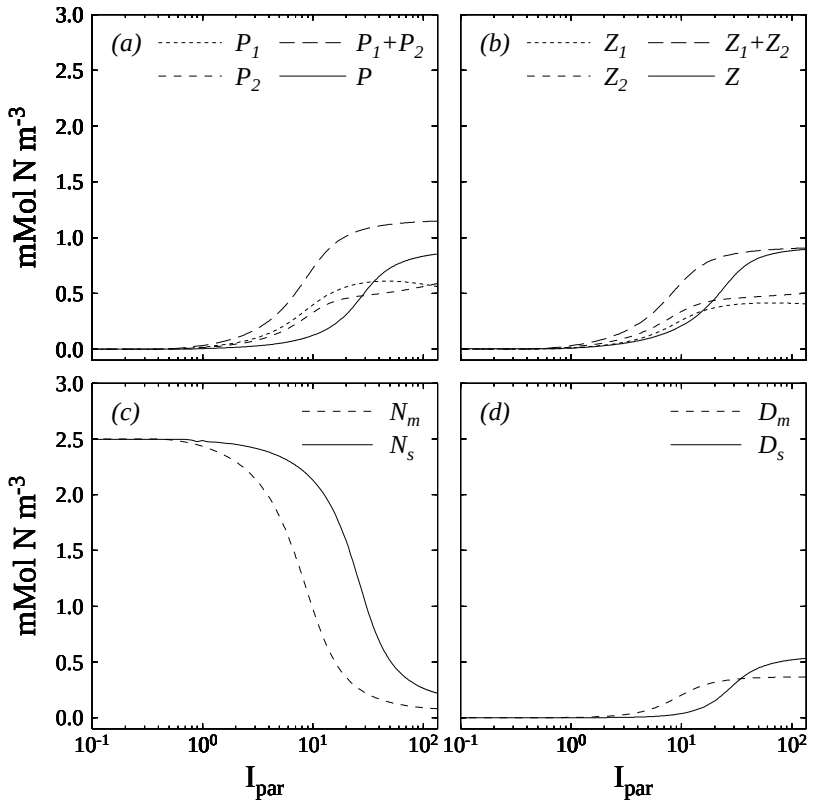

Figure 18: Position of equilibrium points of the different compartments in the NPPZZD and NPZD models, with variable preferences, as function of light availability (photosynthetically available radiation, I_{par}) for $N_0 = 2.5$ mMol N m^{-3}. Single-species model: dissolved nitrogen (N_s), phytoplankton (P), zooplankton (Z), and detritus (D_s). NPPZZD model: small phytoplankton (P_1), large phytoplankton (P_2), total phytoplankton (P_1+P_2), small zooplankton (Z_1), large zooplankton (Z_2), total zooplankton (Z_1+Z_2), detritus (D_m), and dissolved nutrients (N_m). Units are W m^{-2} (I_{par}) and mMol N m^{-3}.

Table I: Parameter values and definitions for NPZD model.

Parameter	Value (units)	Definition
I_0	230 (W m^{-2})	Light intensity at surface.
θ	0.45	PAR fraction of total irradiance.
α	0.025 (mMol N (mg Chl)$^{-1}$ day^{-1} m^2 W^{-1})	Initial slope of the $P-I$ curve.
λ	0.035 (m^{-1})	Light attenuation coefficient.
u_{max}	2.0 (day^{-1})	Phytoplankton maximum growth rate.
g	1.0 (day^{-1})	Zooplankton maximum growth rate.
s	0.01 (day^{-1})	Phytoplankton mortality term.
d	0.1 ([mMol N m^{-3} day]$^{-1}$)	Zooplankton mortality.
e	0.25 (day^{-1})	Remineralization rate for detritus.
a	0.8	Zooplankton assimilation efficiency.
m	0.25	Zooplankton metabolic efficiency.
K_P	0.6 (mMol N m^{-3})	Half-saturation constant for phytoplankton.
K_Z	1.0 (mMol N m^{-3})	Half-saturation constant for zooplankton.
$[chl:N]$	1.0 (mg Chl (mMol N)$^{-1}$)	Chlorophyll to nitrogen ratio.
ϕ_P	0.8	Preference of zooplankton for phytoplankton.
ϕ_D	0.2	Preference of zooplankton for detritus.

Table II: Parameter values and definitions for NPPZD model

Parameter	Value (units)	Definition
I_0	230 (W m^{-2})	Light intensity at surface.
θ	0.45	PAR fraction of total irradiance.
α_1	0.05 (mMol N (mg Chl)$^{-1}$ day^{-1} m^2 W^{-1})	Initial slope of the small phytoplankton $P-I$ curve
α_2	0.025 (mMol N (mg Chl)$^{-1}$ day^{-1} m^2 W^{-1})	Initial slope of the large phytoplankton $P-I$ curve
λ	0.035 (m^{-1})	Light attenuation coefficient.
$u_{1_{max}}$	2.75 (day^{-1})	Small phytoplankton maximum growth rate.
$u_{2_{max}}$	2.0 (day^{-1})	Large phytoplankton maximum growth rate.
g	1.0 (day^{-1})	Zooplankton maximum growth rate.
s_1	0.02 (day^{-1})	Small phytoplankton mortality term.
s_2	0.01 (day^{-1})	Large phytoplankton mortality term.
d	0.1 ([mMol N m^{-3} day]$^{-1}$)	Zooplankton mortality.
e	0.25 (day^{-1})	Remineralization rate for detritus.
a	0.8	Zooplankton assimilation efficiency.
m	0.25	Zooplankton metabolic efficiency.
K_{P_1}	0.4 (mMol N m^{-3})	Half-saturation constant for small phytoplankton.
K_{P_2}	0.6 (mMol N m^{-3})	Half-saturation constant for large phytoplankton.
K_Z	1.0 (mMol N m^{-3})	Half-saturation constant for zooplankton.
$[chl:N]$	1.0 (mg Chl (mMol N)$^{-1}$)	Chlorophyll to nitrogen ratio.
ϕ_{P_1}	0.6	Preference of zooplankton for small phytoplankton.
ϕ_{P_2}	0.3	Preference of zooplankton for large phytoplankton.
ϕ_D	0.1	Preference of zooplankton for detritus.

Table III: Parameter values and definitions for NPPZZD model

Parameter	Value (units)	Definition
I_0	230 (W m^{-2})	Light intensity at surface.
θ	0.45	PAR fraction of total irradiance.
α_1	0.05 (mMol N (mg Chl)$^{-1}$ day^{-1} m^2 W^{-1})	Initial slope of the small phytoplankton $P-I$ curve
α_2	0.025 (mMol N (mg Chl)$^{-1}$ day^{-1} m^2 W^{-1})	Initial slope of the large phytoplankton $P-I$ curve
λ	0.035 (m^{-1})	Light attenuation coefficient.
$u_{1_{max}}$	2.75 (day^{-1})	Small phytoplankton maximum growth rate.
$u_{2_{max}}$	2.0 (day^{-1})	Large phytoplankton maximum growth rate.
g_1	1.5 (day^{-1})	Small zooplankton maximum growth rate.
g_2	1.0 (day^{-1})	Large zooplankton maximum growth rate.
s_1	0.02 (day^{-1})	Small phytoplankton mortality term.
s_2	0.01 (day^{-1})	Large phytoplankton mortality term.
d_1	0.2 ([mMol N m^{-3} day]$^{-1}$)	Small zooplankton mortality.
d_2	0.1 ([mMol N m^{-3} day]$^{-1}$)	Large zooplankton mortality.
e	0.25 (day^{-1})	Remineralization rate for detritus.
a_1	0.85	Small zooplankton assimilation efficiency.
a_2	0.75	Large zooplankton assimilation efficiency.
m_1	0.3	Small zooplankton metabolic efficiency.
m_2	0.2	Large zooplankton metabolic efficiency.
K_{P_1}	0.4 (mMol N m^{-3})	Half-saturation constant for small phytoplankton.
K_{P_2}	0.6 (mMol N m^{-3})	Half-saturation constant for large phytoplankton.
K_{Z_1}	0.75 (mMol N m^{-3})	Half-saturation constant for small zooplankton.
K_{Z_2}	1.0 (mMol N m^{-3})	Half-saturation constant for large zooplankton.
$[chl:N]$	1.0 (mg Chl (mMol N)$^{-1}$)	Chlorophyll to nitrogen ratio.
ϕ_{P_1}	0.7	Preference of small zooplankton for small phytoplankton.
ϕ_{D_1}	0.3	Preference of small zooplankton for detritus.
ϕ_{P_2}	0.45	Preference of large zooplankton for large phytoplankton.
ϕ_{Z_1}	0.45	Preference of large zooplankton for small zooplankton.
ϕ_{D_2}	0.1	Preference of large zooplankton for detritus.